A General Method for Constructing and Searching Conformations in Molecular Rings: From Cremer–Pople Coordinates to 3D Geometries

Anxo Lema-Saavedra[1] and Antonio Fernández-Ramos[1,2]
[1)]*Centro Singular de Investigación en Química Biolóxica e Materiais Moleculares (CIQUS), C/ Jenaro de la Fuente s/n, Universidade de Santiago de Compostela, 15782 Santiago de Compostela, Spain*
[2)]*Departamento de Química Física, Avda. das Ciencias s/n, Universidade de Santiago de Compostela,15782 Santiago de Compostela, Spain*

(*Electronic mail: qf.ramos@usc.es)

(Dated: 27 January 2026)

We present a general framework to construct and systematically search for ring conformations based on Cremer−Pople (CP) coordinates. To our knowledge, this is the first algorithm that provides reasonable ring geometries across different ring sizes from arbitrary CP coordinates. A two-stage ring reconstruction algorithm (RRA) is proposed: (i) projecting the molecule in the *xy* plane and enforcing ring closure while preserving bond lengths, and (ii) redistributing angular distortions across the ring via constrained minimization to achieve chemically viable conformations. The approach is extended to rings with rigid (multiple) bonds through a rigorous ring-reduction scheme that lowers puckering dimensionality and incorporates local stiffness via adjustable parameters, allowing for straightforward recovery of the full structure. In addition, the positions of the substituents attached to the ring are deduced from invariant local references. To systematically explore the conformational space, we formulate a preconditioned sampling of CP amplitudes as a function of hyperspherical coordinates. Additionally, the concept of basis conformations is examined to ensure the unambiguous identification of conformers. Applications to saturated and unsaturated rings with up to eight atoms at the ωB97X-D/def2-TZVPP level demonstrate accurate recovery and classification of known conformers, including correct symmetry multiplicities. Overall, this framework offers a robust and general route to generate high-quality starting geometries for subsequent electronic structure optimizations, while facilitating efficient exploration of puckering space.

I. INTRODUCTION

Flexible molecules can adopt multiple conformations due to high-amplitude internal motions and low potential energy barriers. These motions arise from rotations about single bonds and from puckering in flexible rings.[1–9] The generation of different conformations in acyclic molecules with internal rotors is relatively straightforward because there is a direct relationship between torsion in a single bond and the dihedral angle, which typically varies between 0 and 360°. By contrast, ring puckering is a collective motion that cannot be directly associated with any single dihedral angle. Consequently, changing one dihedral within a ring without adjustments to other internal coordinates can produce geometries that compromise the ring structure.

Kilpatrick, Pitzer, and Spitzer[10] carried out a pioneering work that provided the first mathematical representation of ring conformations, specifically focusing on cyclopentane, which is essential for understanding these complexities. Their work established that cyclopentane can adopt envelope and twisted-boat conformations, which interconvert via pseudorotation described by a distortion amplitude and a phase angle. This approach was extended to six-membered rings by Strauss and Pickett,[11] who highlighted the increased complexity and variety of possible conformers. They emphasized the limitations of using simple dihedral angles for cyclic systems and explored symmetry coordinates and group theory methods to analyze cycloalkanes.[12]

A major advance came with the introduction of the Cremer−Pople (CP) coordinates,[13] which provide a general mathematical framework for describing ring puckering in rings of any size. CP coordinates define a mean plane and express out-of-plane atomic displacements as a set of puckering amplitudes and phase angles, offering $N-3$ independent coordinates for an N-membered ring.[14] They begin by defining a mean plane through the geometric center of the ring such that the perpendicular distances of the N ring atoms balance over the two faces of the plane. The puckering coordinates are related to the displacements, z_j, from the reference plane by

$$q_{\rm m}\cos\phi_{\rm m} = \sqrt{\frac{2}{N}}\sum_{j=1}^{N} z_j \cos(2\pi m(j-1)/N) \qquad (1)$$

$$q_{\rm m}\sin\phi_{\rm m} = \sqrt{\frac{2}{N}}\sum_{j=1}^{N} z_j \sin(2\pi m(j-1)/N), \qquad (2)$$

where $m = 2,3,...,M$ up to $M=(N-1)/2$ if N is odd and up to $M=\frac{1}{2}N-1$ if N is even, $q_{\rm m}\geq 0$ is the puckering amplitude, i. e., the displacement of the nuclei from the mean plane, and $\phi_{\rm m}=[0,2\pi)$ is a phase angle associated with the point of the ring where the distortion is centered. If N is even, there is an additional puckering coordinate for the value $m=N/2$ which defines a symmetric distortion

$$q_{\rm N/2} = \sqrt{\frac{1}{N}}\sum_{j=1}^{N} z_j \cos[(j-1)\pi] = \sqrt{\frac{1}{N}}\sum_{j=1}^{N}(-1)^{j-1} z_j, \quad (3)$$

where $q_{\rm N/2}$ is an amplitude that, in contrast to $q_{\rm m}$, can be negative or positive, and is associated with alternating positive and negative signs in adjacent out-of-plane coordinates

($\mp z_j = \pm z_{j+1}$). The puckering coordinates of Eqs. 1 and 2 (plus eq 3 for N even) can be employed to describe the conformation of any ring. The inverse relation between coordinates is exact and is given by

$$z_j = \sqrt{\frac{2}{N}} \sum_{m=2}^{M} q_m \cos(\phi_m + 2\pi m(j-1)/N); \quad N \text{ odd} \tag{4}$$

$$\begin{aligned} z_j =& \sqrt{\frac{2}{N}} \sum_{m=2}^{M} q_m \cos(\phi_m + 2\pi m(j-1)/N) \\ &+ \sqrt{\frac{1}{N}} q_{\mathrm{N}/2}(-1)^{j-1}; \quad N \text{ even} \end{aligned} \tag{5}$$

By orthogonality of the trigonometric basis, the total puckering amplitude Q is given by

$$Q^2 = \sum_{\mathrm{m}} q_{\mathrm{m}}^2 = \sum_{j=1}^{N} z_j^2. \tag{6}$$

The total number of puckering coordinates is $N-3$, so four-membered rings have only one puckering coordinate, which is given by the amplitude q_2 of Eq. (3). In this case, only the last term on the right-hand side of Eq. (5) contributes, and $z_1 = -z_2 = z_3 = -z_4$ and the substitution into Eq. (3) leads to $q_2 = \pm 2z_1$. For a five-member ring, there is just one set of two amplitude-phase coordinates (q_2, ϕ_2). These equations can be used as a first step in conformational searches. The procedure of obtaining the CP coordinates from a given structure, modifying their values, recovering the new z_j, and setting up the Cartesian coordinates seems to be an ideal way to generate different conformations of a cyclic molecule.

Nevertheless, reconstructing chemically meaningful Cartesian coordinates from a modified set of CP coordinates is nontrivial because CP coordinates provide information only on the out-of-plane elevations (or, equivalently, of the puckering subspace), i.e., on N Cartesian coordinates or $N-3$ internal coordinates, whereas a full 3D ring geometry requires $3N$ Cartesian coordinates or $3N-6$ internal degrees of freedom. In practice, specifying a new set of z_j values (via the inverse CP relation) does not uniquely define the in-plane x_j, y_j coordinates, and attempting to retain the original ones distorts bond lengths and bond angles, or even compromises the ring integrity. This underdetermination is the main obstacle to using CP coordinates as reconstruction variables for conformational searches.

This issue was noticed by Petit *et al.*,[15] who argued that transforming between CP and Cartesian coordinates can distort bond lengths/angles; Cremer replied[16] that while CP coordinates are mathematically rigorous descriptors, the reconstruction problem requires additional constraints. Cremer subsequently proposed a procedure that uses bond lengths and angles from a reference geometry to rebuild a ring from a target set of $\{z_j\}$ values.[17] However, because the distortion is concentrated on a limited subset of internal angles, the resulting in-plane geometry can be quite heterogeneous when the new CP coordinates differ substantially from the reference. In these cases the method may yield unrealistic angles and, for sufficiently large distortions, it may fail to produce a closed ring.

Prior to the work of Cremer and Pople, other significant contributions to the field include the work of Geise *et al.*[18] and Altona *et al.*,[19] who developed methods for describing ring puckering in fused and substituted rings, emphasizing the importance of considering the interactions between adjacent rings and substituents. Altona and Sundaralingam[20] further refined the analysis of five-membered rings, developing improved methods for calculating puckering coordinates and demonstrating their relevance in nucleosides and nucleotides. However, their approach relies on a truncated Fourier series approximation using a single cosine function, which is not exact. Consequently, the distortion amplitude is dependent on the atom numbering in the ring, potentially affecting the accuracy of the conformational representation.

Continuing in the framework of CP coordinates, Boeyens and Evans[21–23] extended the work of Pickett and Strauss,[12] exploring symmetry coordinates and group theory approaches to ring analysis in cycloalkanes, providing alternative mathematical perspectives. Zefirov, Palyulin, and coworkers[24,25] recommended a set of coordinates that also define pairs of amplitude-phase coordinates, and sometimes offer advantages in specific contexts.[26] The difference lies in the fact that these coordinates do not describe out-of-plane movements but rather changes in dihedral angles. Their method substitutes the elevations in the plane with the sine of half the torsion angle. In some cases this is a fairly good approximation, but the error increases with the amplitude of the distortion.

Alonso-Gil[27] designed an algorithm and its code, *Monte-Carbo*, to study five- to seven-membered rings. The method employs a combination of generalized internal coordinates to define the geometry and uses a pseudo-random number generator for the conformational search. However, the program lacks an internal mechanism to assess the physical reliability of generated structures or to prevent chemical changes during the optimization process. Therefore, a post-analysis is necessary to verify and eliminate any incorrect configurations. Other authors[28,29] have directly used CP coordinates for small member rings or employed conformational sampling schemes based on canonical conformations.[30] Zou *et al.*[31] incorporated ring puckering and deformation coordinates along with analytical gradients,[17] which may improve the efficiency of geometry optimizations. All this previous research has significantly improved our understanding of ring flexibility and has provided a solid foundation for precise conformational analysis in computational chemistry.

However, despite substantial progress in describing and analyzing ring puckering, a general constructive algorithm that maps arbitrary CP coordinates to chemically viable Cartesian structures across ring sizes has not been available. Here we present, to our knowledge, the first general algorithm that generates chemically consistent conformations for any reasonable set of CP coordinates, preserving structural integrity while systematically exploring the puckering-coordinate phase space.

This objective is organized throughout the manuscript as

follows: the methodology section introduces an approach for constructing rings based on specified CP coordinates, representing a generalization of the algorithm developed by Cremer.[17] It also details how this method can be adapted to include partially unsaturated (rigid-bond) rings. Once the desired conformation is established, we outline the process for placing substituents to facilitate subsequent electronic structure optimization. Finally, we propose a preconditioned sampling of the conformational space using hyperspherical coordinates. This methodology is applied to various ring systems in the results section, followed by a conclusion that summarizes our findings.

II. METHODOLOGY

A. Ring condition equation

To set up the problem, an initial or reference geometry is considered, with coordinates labeled by a superscript $\circ$ to distinguish them from the newly generated geometry. This reference geometry can be a previously optimized conformer or any ring structure with reasonable geometric parameters for the system under study. The first step involves removing all substituents from the ring, leaving just the closed structure composed of N atoms (or nodes) numbered consecutively as $j = 1,2,3,\ldots,N$. The reference bond lengths r_j° correspond to the distances between atoms j and $j-1$, except for r_1°, which is the distance between the first atom ($j = 1$) and the last atom ($j = N$). The reference bond angles θ_j° involve atoms $j-2$, $j-1$, and j, with θ_1° and θ_2° defined by atoms $(N-1,N,1)$ and $(N,1,2)$, respectively. Finally, the reference dihedrals φ_j° involve atoms $j-3$, $j-2$, $j-1$, and j, with φ_1°, φ_2°, and φ_3° defined by atoms $(N-2,N-1,N,1)$, $(N-1,N,1,2)$, and $(N,1,2,3)$, respectively. For the construction of the ring or any other chemical structure $3N-6$ of these internal coordinates are needed, for instance $N-1$ bond lengths given by the set $\{r_j^\circ | j = 2,3,\ldots,N\}$, $N-2$ bond angles given by $\{\theta_j^\circ | j = 3,4,\ldots,N\}$, and $N-3$ dihedral angles given by $\{\varphi_j^\circ | j = 4,5,\ldots,N\}$.

A possible construction of the ring geometry could be to place the first atom at the origin, the second atom is placed in the positive direction of the x axis, so the position vector, $\mathbf{r}_2^\circ$, is a three-dimensional column vector with the distance r_2° as the first element and zero on the others. The third atom is placed relative to atom $j = 2$ and rotated about the z axis by the supplementary angle of the bond angle, i.e., $\bar{\theta}_3^\circ = \pi - \theta_3^\circ$. The rotation can be achieved using the matrix

$$\mathscr{R}_z(\theta_j) = \begin{pmatrix} \cos(\theta_j) & \sin(\theta_j) & 0 \\ -\sin(\theta_j) & \cos(\theta_j) & 0 \\ 0 & 0 & 1 \end{pmatrix} \tag{7}$$

and taking into account that

$$\mathscr{R}_z(\bar{\theta}_j) = \mathscr{R}_z(\pi - \theta_j) = [\mathscr{R}_z(\theta_j)]^{\mathrm{T}} \mathscr{R}_z(\pi), \tag{8}$$

where $(\,)^{\mathrm{T}}$ denotes the transpose of a given vector or matrix. The position vector $\mathbf{R}_3^\circ$, of atom $j = 3$ is given by

$$\mathbf{R}_3^\circ = \mathscr{R}_z(\bar{\theta}_3^\circ)\mathbf{r}_3^\circ + \mathbf{R}_2^\circ \tag{9}$$

where $\mathbf{R}_2^\circ = \mathbf{r}_2^\circ$.

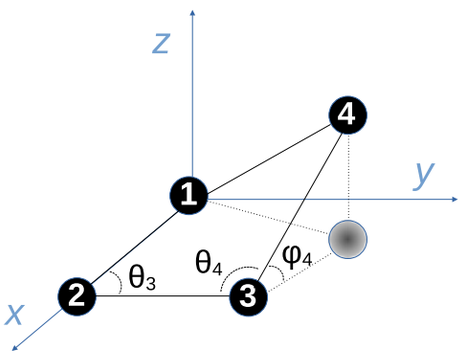

FIG. 1. Construction of a four-membered ring employing internal coordinates.

The atom $j = 4$ should be rotated about the z axis first and then an angle φ_4° with respect to the x axis (shown in Figure 1). The rotation matrix in this case is

$$\mathscr{R}_x(\varphi_j) = \begin{pmatrix} 1 & 0 & 0 \\ 0 & \cos(\varphi_j) & -\sin(\varphi_j) \\ 0 & \sin(\varphi_j) & \cos(\varphi_j) \end{pmatrix} \tag{10}$$

and the position vector is

$$\mathbf{R}_4^\circ = \mathscr{R}_z(\bar{\theta}_3^\circ)\mathscr{R}_x(\varphi_4^\circ)\mathscr{R}_z(\bar{\theta}_4^\circ)\mathbf{r}_4^\circ + \mathbf{R}_3^\circ. \tag{11}$$

Extending Eq. (11) to the last atom of the ring, we obtain that

$$\mathbf{R}_{\mathrm{N}}^\circ = \mathscr{R}_z(\bar{\theta}_3^\circ) \prod_{j=4}^{\mathrm{N}} \mathscr{R}_x(\varphi_j^\circ)\mathscr{R}_z(\bar{\theta}_j^\circ)\mathbf{r}_j^\circ + \mathbf{R}_{\mathrm{N}-1}^\circ. \tag{12}$$

By definition the above internal coordinates form a ring, and therefore

$$(\mathbf{R}_{\mathrm{N}}^\circ)^{\mathrm{T}}\mathbf{R}_{\mathrm{N}}^\circ = (r_1^\circ)^2. \tag{13}$$

It can be shown that the combination of Eqs. (12) and (13) leads to

$$(r_1^\circ)^2 = \sum_{i=2}^{N} (r_i^\circ)^2 + 2\sum_{j=2}^{i-1} (\mathbf{r}_j^\circ)^{\mathrm{T}} \left(\prod_{k=j+1}^{i} \mathbf{M}_k \right) \mathbf{r}_i^\circ, \tag{14}$$

where $\mathbf{M}_k$ is

$$\mathbf{M}_k = \begin{cases} \mathscr{R}_x(\varphi_k^\circ)\mathscr{R}_z(\bar{\theta}_k^\circ), & k > 3 \\ \mathscr{R}_z(\bar{\theta}_k^\circ), & k = 3. \end{cases} \tag{15}$$

Taking into account that the vectors $\mathbf{r}_j^{\circ}$ only contain the bond distance in the first element and the other elements are zero, Eq. (14) can be written as

$$(r_1^{\circ})^2 = \sum_{i=2}^{N}(r_i^{\circ})^2 + 2\sum_{j=2}^{i-1} r_j^{\circ} r_i^{\circ}\,\mathrm{Tr}\left(\mathbf{P}_1 \prod_{k=j+1}^{i} \mathbf{M}_k\right), \tag{16}$$

where

$$\mathbf{P}_1 = \mathbf{e}_1\mathbf{e}_1^{\mathrm{T}} \tag{17}$$

is a projection matrix, $\mathbf{e}_1$ is the column vector with $\mathbf{e}_1^{\mathrm{T}} = (1,0,0)$, and Tr( ) denotes the trace of the matrix, which in this case is the scalar equal to the (1,1) element of the matrix product.

Equation (16) establishes the ring-closure condition and serves as the basis for our search over conformations. The closure constraints induce strong coupling among internal coordinates, making naive modifications of torsions likely to break the ring or yield unrealistic structures.

B. Ring reconstruction algorithm (RRA)

The reference geometry contains a set of bond distances, bond angles, and dihedral angles $\{r_j^{\circ}, \theta_j^{\circ}, \varphi_j^{\circ}\}$ that can be transformed into a set of projected bond distances, angles, and elevations $\{s_j^{\circ}, \alpha_j^{\circ}, z_j^{\circ}\}$, as the values of z_j° can be obtained from the distances to the mean plane.

The mean plane for any ring geometry $\{r_j, \theta_j, \varphi_j\}$, whose geometrical center lies in the origin of coordinates, and with a set of position vectors $\{\mathbf{R}_j\}$, which is not necessarily the reference geometry, can be determined from the cross product of the vectors

$$\mathbf{R}' = \sum_{j=1}^{N} \mathbf{R}_j \sin\left(\frac{2\pi(j-1)}{N}\right), \tag{18}$$

and

$$\mathbf{R}'' = \sum_{j=1}^{N} \mathbf{R}_j \cos\left(\frac{2\pi(j-1)}{N}\right). \tag{19}$$

Specifically, the unit vector perpendicular to the mean plane is

$$\hat{\mathbf{n}} = \frac{\mathbf{R}' \times \mathbf{R}''}{\|\mathbf{R}' \times \mathbf{R}''\|}, \tag{20}$$

and the values of z_j are simply

$$z_j = \mathbf{R}_j \cdot \hat{\mathbf{n}}. \tag{21}$$

The projected internal coordinates $\{s_j, \alpha_j\}$ relate to the unprojected quantities $\{r_j, \theta_j\}$ by

$$s_j = \sqrt{r_j^2 - (z_j - z_{j-1})^2}, \tag{22}$$

and

$$\cos(\alpha_j) = \frac{2r_{j-1}r_j\cos(\theta_j) + \zeta_j}{2s_{j-1}s_j}, \tag{23}$$

where

$$\zeta_j = (z_j - z_{j-2})^2 - (z_j - z_{j-1})^2 - (z_{j-1} - z_{j-2})^2. \tag{24}$$

Note that the three-dimensional ring structure can be reoriented so that the *xy* plane coincides with the mean plane. Consequently, the condition of Eq. (16) is also satisfied by the projection onto the *xy* plane, as the reference geometry can be recovered by adding back the z_j° values. The projected version of Eq. (16) is

$$g(\boldsymbol{\alpha}^{\circ}) = \sum_{i=2}^{N}(s_i^{\circ})^2 + 2\sum_{j=2}^{i-1} s_j^{\circ} s_i^{\circ}\,\mathrm{tr}\left(\mathbf{P}_1 \prod_{k=j+1}^{i} \mathbf{S}_k^{\circ}\right)(s_1^{\circ})^2 = 0, \tag{25}$$

where

$$\mathbf{S}_k^{\circ} = [\mathscr{R}_z(\alpha_k^{\circ})]^{\mathrm{T}}\mathscr{R}_z(\pi), \tag{26}$$

and $\boldsymbol{\alpha}^{\circ} = \{\alpha_j^{\circ} | j = 3,4,\ldots,N\}$. Here, we have employed Eq. (8) but for the in-plane angles, instead of the bond angles.

When the elevations are modified relative to the reference geometry to generate a different conformation, the distances and angles must adjust to accommodate the new values of z_j. In this new scenario, the in-plane angles and the bond-length projections shift from the reference values. When the new sets of $\boldsymbol{\alpha} = \{\alpha_j | j = 3,4,\ldots,N\}$ and $\{s_j, z_j\}$ are substituted into Eq. (25), the closure condition is no longer satisfied, and

$$g(\boldsymbol{\alpha}) \neq 0. \tag{27}$$

The RRA algorithm keeps the set of distances $\{r_j^{\circ}\}$ invariant with respect to the reference values while changing the bond angles. That is, the new ring conformation will be described by the set $\{s_j, \alpha_j, z_j\}$. Notice that, even if the distances are invariant, the projections of the bond distances s_j differ from those in the reference s_j° because of the new set $\{z_j\}$ which is different from $\{z_j{}^{\circ}\}$ by virtue of Equation (22). This is easily shown in cyclobutane (Appendix B).

As a first step, the new values of the set $\boldsymbol{\alpha}$ should be chosen to either find the roots of Eq. (27) or minimize the squared function

$$[g(\boldsymbol{\alpha})]^2 = \left[\sum_{i=2}^{N}(s_i)^2 + 2\sum_{j=2}^{i-1} s_j s_i\,\mathrm{Tr}\left(\mathbf{P}_1 \prod_{k=j+1}^{i} \mathbf{S}_k\right) - (s_1)^2\right]^2. \tag{28}$$

We found that a much better initial guess for $\boldsymbol{\alpha}^{\circ}$ is not the in-plane angles of the reference geometry, but rather the set of angles of a regular N-gon, i.e. those given by $\boldsymbol{\alpha}^{\circ} = \{\alpha_j^{\circ} = \frac{(N-2)\cdot\pi}{N} \mid j = 3,4,\ldots,N\}$. The initial structure with these in-plane angles is always an open ring. Equation (28) always exists provided that $|z_j - z_{j-1}| < r_j^{\circ}$ and ensures that at the end of the minimization the ring is closed, although this first

minimization procedure may lead to some odd in-plane angles. This optimization step can be carried out employing a gradient descent algorithm.[32,33]

As a second step, the optimal values of α_j obtained in the first step are transformed into three-dimensional θ_j angles, which are then used as initial input. The new objective is to ensure that the bond angles remain close to their reference values, maintaining bond lengths and elevations constant.

One way to achieve this is by minimizing the quadratic (harmonic) function

$$f(\boldsymbol{\theta}) = \gamma_1 \left[\theta_1(\boldsymbol{\theta}) - \theta_1^{\mathrm{o}}\right]^2 + \gamma_2 \left[\theta_2(\boldsymbol{\theta}) - \theta_2^{\mathrm{o}}\right]^2 + \sum_{j=3}^{N} \gamma_j \left(\theta_j - \theta_j^{\mathrm{o}}\right)^2, \tag{29}$$

where γ_j acts as a force constant associated with the stiffness of each bond angle. To obtain a reasonable structure, the function to be minimized should include all N bond angles, i.e., θ_1, θ_2, and $\boldsymbol{\theta} = \{\theta_j \mid j = 3,4,\ldots,N\}$, although θ_1 and θ_2 are not independent since both depend on the θ_j. In fact there is an additional dependent angle, which can be any of the remaining θ_j because all the bond distances are known. The same also holds for α_1, α_2, which are function of $\boldsymbol{\alpha}$. In particular,

$$\alpha_1(\boldsymbol{\alpha}) = \arccos\left\{\left[(s_{\mathrm{N}})^2 + \sum_{j=2}^{\mathrm{N}-1} s_j s_{\mathrm{N}} \,\mathrm{Tr}\left(\mathbf{P}_1 \prod_{k=j+1}^{\mathrm{N}} \mathbf{S}_k\right)\right] \frac{1}{s_1 s_{\mathrm{N}}}\right\}, \tag{30}$$

and

$$\alpha_2(\boldsymbol{\alpha}) = \arccos\left\{\left[(s_2)^2 + \sum_{j=3}^{\mathrm{N}} s_2 s_j \,\mathrm{Tr}\left(\mathbf{P}_1 \prod_{k=3}^{j} \mathbf{S}_k\right)\right] \frac{1}{s_1 s_2}\right\}, \tag{31}$$

where $\mathbf{S}_k$ is given by Eq. (26) but for the angles obtained in the first step of the optimization. We can still employ the in-plane angles to minimize the function of Eq. (29), which is a function of the three-dimensional angles, because of the relation among them given by Eq. (23) is

$$\cos(\theta_j) = \frac{2 s_{j-1} s_j \cos(\alpha_j) - \zeta_j}{2 r_{j-1} r_j}. \tag{32}$$

Using Eq. (32) to express each θ_j in terms of α_j, and then incorporating them into Eq. (29), one obtains

$$f(\boldsymbol{\alpha}) = \sum_{j=1}^{N} \gamma_j \left[\arccos\left(\frac{2 s_j s_{j-1} \cos(\alpha_j) - \zeta_j}{2 r_j^{\mathrm{o}} r_{j-1}^{\mathrm{o}}}\right) - \theta_j^{\mathrm{o}}\right]^2, \tag{33}$$

where $\alpha_1 = \alpha_1(\boldsymbol{\alpha})$ and $\alpha_2 = \alpha_2(\boldsymbol{\alpha})$ are given by Eqs. (30) and (31), respectively. Equation (33) can be approximated under the assumption that the terms $\xi_j = (\theta_j - \theta_j^{\mathrm{o}})$ are small. Specifically, if we consider that

$$\cos(\theta_j) = \cos(\theta_j^{\mathrm{o}} + \xi_j) \approx \cos(\theta_j^{\mathrm{o}}) - \xi_j \sin(\theta_j^{\mathrm{o}}) \tag{34}$$

and equate Eq. (34) to Eq. (32), the function of Eq. (33) becomes

$$f(\boldsymbol{\alpha}) = \sum_{j=1}^{\mathrm{N}} \gamma_j \left(\frac{\cos(\theta_j^{\mathrm{o}})}{\sin(\theta_j^{\mathrm{o}})} - \frac{2 s_j s_{j-1} \cos(\alpha_j) - \zeta_j}{2 r_j^{\mathrm{o}} r_{j-1}^{\mathrm{o}} \sin(\theta_j^{\mathrm{o}})}\right)^2. \tag{35}$$

This is a reasonable approximation because the deviation with respect to the reference angle changes slowly as shown in Figure 11.

Therefore, the problem reduces to minimizing the function of Eq. (35) subject to the constraint imposed by Eq. (25) but with angles α_j instead of α_j^{o}. This is equivalent to minimize the Lagrangian

$$\mathscr{L}(\boldsymbol{\alpha}, \lambda) = f(\boldsymbol{\alpha}) + \lambda \; g(\boldsymbol{\alpha}), \tag{36}$$

where λ is a Lagrange multiplier and $g(\boldsymbol{\alpha}) = 0$ is the constraint. The minimum of function $f(\boldsymbol{\alpha})$ can be achieved by solving the following system of equations

$$\begin{cases} \dfrac{\partial \mathscr{L}}{\partial \lambda} = g(\boldsymbol{\alpha}) = 0 \\ \\ \dfrac{\partial \mathscr{L}}{\partial \alpha_j} = 0 \quad ; \quad j = 3,4,\ldots,N \end{cases} \tag{37}$$

Equation (37) can be solved using a sequential least squares programming (SLSQP) algorithm as implemented in SciPy.[34] Once the optimal in-plane angles are obtained, the three-dimensional ring geometry is readily obtained by adding the z_j Cartesian coordinates to the planar structure.

C. Rings with rigid bonds

Cremer−Pople coordinates retain limited structural information about the molecule and were not designed to handle rigid bonds within the ring. Applying them directly in molecules with multiple bonds tends to distort the structure of the rigid region. To address this, we adopt a ring-reduction strategy that lowers the puckering dimensionality while incorporating local stiffness.

When a double bond connects atoms 1 and 2, as in Figure 2, this pair is replaced by its midpoint m. This reduces the ring size by one atom and decreases the number of CP coordinates by one, consistent with reported behavior of cycloalkenes (e.g., cyclopentene acting as a four-membered ring and cycloheptene as a six-membered ring).[35–38]

For cyclohexene, the midpoint substitution yields a pentane-like reduced structure with reference distances r_{6m}^{o} and r_{m3}^{o} (together with r_4^{o}, r_5^{o}, and r_6^{o}). The reduced CP coordinates (q_2, ϕ_2) are obtained as described previously using these geometric references.

To preserve the double-bond environment during optimization, we fix r_{6m}^{o}, r_{m3}^{o}, and the angle $\theta_{6m3}^{\mathrm{o}}$. RRA supports fixed distances and can penalize angular changes by adjusting the coefficient γ in Eq. (29). If all atoms in the ring are equivalent the value of γ is arbitrary, for instance $\gamma_j = 1$ may correspond to standard flexibility of a single bond, while $\gamma > 1$ indicates increasing stiffness; we find that $\gamma = 10$ reproduces the rigidity of double bonds well. Combined with the reduced ring dimensionality, this induces a block-like motion of atoms 6 and 1–3 during puckering. After modifying the reduced CP

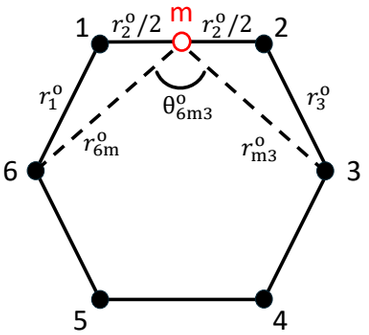

FIG. 2. Definition of coordinates around the double bond in cyclohexene.

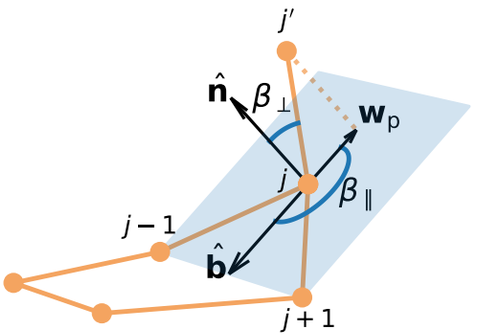

FIG. 3. Definition of vectors for substituent positioning.

coordinates, the original cyclohexene structure is recovered for electronic-structure optimization.

If a slight variation of θ_{6m3} is allowed (by taking γ closer to one), the final distance r_{36} may differ from its reference r_{36}^o. In that case, reconstruction from the pentane-like form while keeping r_1^o, r_2^o, and r_3^o is achieved by applying Eq. (16) to the four involved atoms. Given r_{36}, the unknowns are the small distortions ξ_2 and ξ_3 of the angles θ_2^o and θ_3^o. The geometric relation is

$$\begin{aligned}&(r_1^o)^2+(r_2^o)^2+(r_3^o)^2-r_{36}^2\\&-2r_1^o r_2^o\cos(\theta_2^o+\xi_2)-2r_2^o r_3^o\cos(\theta_3^o+\xi_3)\\&+2r_1^o r_3^o\cos(\theta_2^o+\xi_2)\cos(\theta_3^o+\xi_3)\\&-2r_1^o r_3^o\sin(\theta_2^o+\xi_2)\sin(\theta_3^o+\xi_3)\cos\varphi_3^o=0.\end{aligned}\tag{38}$$

Assuming small distortions and $\xi_2=\xi_3=\xi$, linearization leads to

$$\xi=-\frac{A}{D},\tag{39}$$

with

$$\begin{aligned}A&=(r_1^o)^2+(r_2^o)^2+(r_3^o)^2-r_{36}^2\\&\quad-2r_1^o r_2^o\cos\theta_2^o-2r_2^o r_3^o\cos\theta_3^o\\&\quad+2r_1^o r_3^o\left[\cos\theta_2^o\cos\theta_3^o-\sin\theta_2^o\sin\theta_3^o\cos\varphi_3^o\right]\\D&=2r_1^o r_2^o\sin\theta_2^o+2r_2^o r_3^o\sin\theta_3^o\\&\quad-2r_1^o r_3^o\sin(\theta_2^o+\theta_3^o)[1+\cos\varphi_3^o].\end{aligned}\tag{40}$$

With this correction, the double bond is reconstructed straightforwardly, and the full cyclohexene geometry is recovered after placing substituents as described below.

D. Substituent positioning relative to ring conformation

The spatial orientation of atoms directly bonded to the ring depends on the specific conformation adopted by the cycle, and the repositioning of ring substituents following modifications of the CP coordinates may be challenging. For example, during the inversion motion of a chair conformation, substituents initially occupying axial positions transition to equatorial positions, and vice versa. In this regard, Cremer[39] performed an analysis of substituent positions based on their angular relationships relative to the mean plane of the ring, revealing characteristic patterns associated with distinct ring conformations. Nevertheless, such analysis proves to be more applicable after full conformational optimization rather than for the initial placement of substituents.

At this stage, a more practical approach is to position the substituents so that their relative placement remains essentially unchanged regardless of the ring conformation. This is important because RRA works on a molecule from which all substituents have been removed, and the objective is to recover the position of the substituents relative to the atoms to which they are bonded, rather than relative to the overall ring conformation, to facilitate subsequent electronic structure optimization.

To achieve this, the following procedure is applied: the substituent atom bonded to atom j is labeled as j', and its position is defined with respect to the plane formed by atoms $j-1$, j, and $j+1$, as well as the normal vector to this plane in the reference geometry (see Figure 3). The following vector definitions as a function of the position vectors of the atoms are useful

$$\mathbf{u}=\mathbf{R}_{j-1}-\mathbf{R}_j,\quad \mathbf{v}=\mathbf{R}_{j+1}-\mathbf{R}_j,\quad \mathbf{w}=\mathbf{R}_{j'}-\mathbf{R}_j.\tag{41}$$

The equations of this section refer to the reference geometry, but for simplicity, we have removed the $\circ$ superscript. The position of j' with respect to the atom j is calculated as the angle between the normal to the plane and vector $\mathbf{w}$. In particular,

$$\beta_\perp=\arccos\left(\frac{\mathbf{w}\cdot\hat{\mathbf{n}}}{\|\mathbf{w}\|}\right),\tag{42}$$

where $\hat{\mathbf{n}}$ is the unit vector normal to the plane. The bisector unit vector that starts at the position of atom j is

$$\hat{\mathbf{b}}=\frac{\hat{\mathbf{u}}+\hat{\mathbf{v}}}{\|\hat{\mathbf{u}}+\hat{\mathbf{v}}\|},\tag{43}$$

where $\hat{\mathbf{u}}$ and $\hat{\mathbf{v}}$ are unit vectors in the direction of $\mathbf{u}$ and $\mathbf{v}$, respectively. The projection of $\mathbf{w}$ onto the plane is

$$\mathbf{w}_\mathrm{p} = \mathbf{w} - (\mathbf{w}\cdot\hat{\mathbf{n}})\hat{\mathbf{n}}, \tag{44}$$

and $\beta_\parallel$ is the angle between $\mathbf{w}_\mathrm{p}$ and the bisector

$$\beta_\parallel = \arccos\left(\frac{\mathbf{w}_\mathrm{p}\cdot\hat{\mathbf{b}}}{\|\mathbf{w}_\mathrm{p}\|}\right). \tag{45}$$

Angles $\beta_\parallel$ and $\beta_\perp$ are employed to find the coordinates of atom j' attached to atom j once the minimization procedure for the new CP coordinates is finished (see Figure 3). Now the input variables are the two angles and the new position vectors $\mathbf{R}_{j-1}$, $\mathbf{R}_j$, and $\mathbf{R}_{j+1}$, which allows finding the new coordinates of atom j'

$$\mathbf{R}_{j'} = \mathbf{R}_j + \|\mathbf{w}\|\left(\hat{\mathbf{w}}_\mathrm{p}\sin\beta_\perp + \hat{\mathbf{n}}\cos\beta_\perp\right), \tag{46}$$

where

$$\hat{\mathbf{w}}_\mathrm{p} = \hat{\mathbf{b}}\cos\beta_\parallel + (\hat{\mathbf{n}}\times\hat{\mathbf{b}})\sin\beta_\parallel, \tag{47}$$

and $\|\mathbf{w}\|$ is the distance between atoms j and j' in the reference geometry. In general, substituents lie approximately in a plane perpendicular to the local ring plane and along the bisector direction. Therefore, atom j' will have a direction close to that of the bisector vector but with opposite orientation, so $\beta_\parallel \approx \pi$, and Eq. (46) simplifies to

$$\mathbf{R}_{j'} \approx \mathbf{R}_j + \|\mathbf{w}\|\left(\hat{\mathbf{n}}\cos\beta_\perp - \hat{\mathbf{b}}\sin\beta_\perp\right). \tag{48}$$

Equation (48) is very simple but provides a good starting point for placing the substituents for the subsequent electronic structure optimization.

E. Conformational search

Equation (37) defines the geometry of the ring based on given CP coordinates. However, it is essential to perform a preconditioned search over different values of the CP coordinates to systematically explore various conformations. For instance, in acyclic molecules, this process resembles initiating a conformational search around a single carbon-carbon bond torsion, considering the two *gauche* and *anti* conformations. In molecular rings, however, identifying a suitable set of preconditioned CP coordinates is more complex, requiring a thorough exploration of the puckering coordinate phase space to uncover diverse conformational possibilities. Thus, systematically exploring the puckering coordinate phase space is our second goal.

Since these coordinates depend on the atom numbering in the ring, we consistently follow IUPAC conventions in this manuscript to ensure consistency and support future comparisons.[40]

For a five-membered ring where the CP coordinates are the pair (q_2,ϕ_2), the amplitude q_2 controls the degree of puckering but does not affect the conformation of the ring, whereas the phase ϕ_2 determines the type of conformation. Therefore all conformations can be obtained just by varying the phase. For cyclopentane, any symmetry-equivalent conformation is obtained by

$$\phi_2 \;=\; \pm\left(\phi_2^0 + \frac{\pi}{N}k\right), \qquad k = 0,\ldots,2N-1, \tag{49}$$

where ϕ_2^0 sets the phase for a given conformation. For instance, $\phi_2^0 = 0$ leads to an envelope representative conformation ^{1}E and $\phi_2^0 = \pi/10$ to a twist representative conformation ^{1}T$_2$. Figure 4 illustrates these conformations.

Notice that E and T are the only cases where all symmetry-equivalent conformations can be generated using only the plus sign in Eq. (49); mapping any other conformation requires also the minus sign. Therefore, there are ten symmetry-equivalent E conformations and ten symmetry-equivalent T conformations (altogether twenty special cases), whereas any other conformation has twenty symmetry equivalents. In particular, every E conformation is followed by another symmetry-equivalent E conformation every $\Delta\phi_2 = \pi/5$ radians, and halfway between them a T conformation appears as indicated in Table I.

TABLE I. Values of q_m for a total amplitude Q and their relation to the hyperspherical angles ψ_1,ψ_2 for $N = 5-8$. For cases with a single nonzero amplitude q_m, the table lists representative conformations at phases ϕ_m^0 . The corresponding pair of basis conformations is obtained from Eq. (C1) using $\phi_m = \phi_m^0$ and $\phi_m = \phi_m^0 + \pi/2$.

N	q_2	q_3	q_4	ψ_1	ψ_2	ϕ_m^0	description
5	Q	—	—	—	—	0	envelope (E)
5	Q	—	—	—	—	$\pi/10$	twist (T)
6	Q	0	—	$\pi/2$	—	0	boat (B)
6	Q	0	—	$\pi/2$	—	$\pi/6$	skew (S)
6	0	$\pm Q$	—	0,π	—	undefined	chair (C)
7	Q	0	—	$\pi/2$	—	0	boat (B)
7	Q	0	—	$\pi/2$	—	$\pi/14$	twist-boat (TB)
7	0	Q	—	0	—	0	chair (C)
7	0	Q	—	0	—	$\pi/14$	twist-chair (TC)
8	Q	0	0	$\pi/2$	$\pi/2$	0	boat-boat (BB)
8	Q	0	0	$\pi/2$	$\pi/2$	$\pi/4$	twist-boat (TB)
8	0	Q	0	0	$\pi/2$	0	long-chair (L)[a]
8	0	Q	0	0	$\pi/2$	$\pi/8$	chair (C)
8	0	0	$\pm Q$	0	0,π	undefined	crown (W)

[a] Cremer[39] indicated that $\phi_3 = 0$ and $\phi_3 = \pi/2$ correspond to different conformations. However, for cyclooctane both structures are equivalent.

Throughout this work, representative conformations are the chemically labeled landmark listed at the conventional phases ϕ_m^0 in Table I. By contrast, for a fixed mode m with a single nonzero amplitude q_m (all other amplitudes set to zero), the two basis conformations associated with a representative phase ϕ_m^0 are the structures generated by Eq. (C1) at $\phi_m = \phi_m^0$ and $\phi_m = \phi_m^0 + \pi/2$. This use of 'representative' is independent of the reference geometry employed by the reconstruction algorithm.

Any intermediate conformation (I) is a linear combination of the two basis functions C_2 and S_2 (see Appendix C), so the

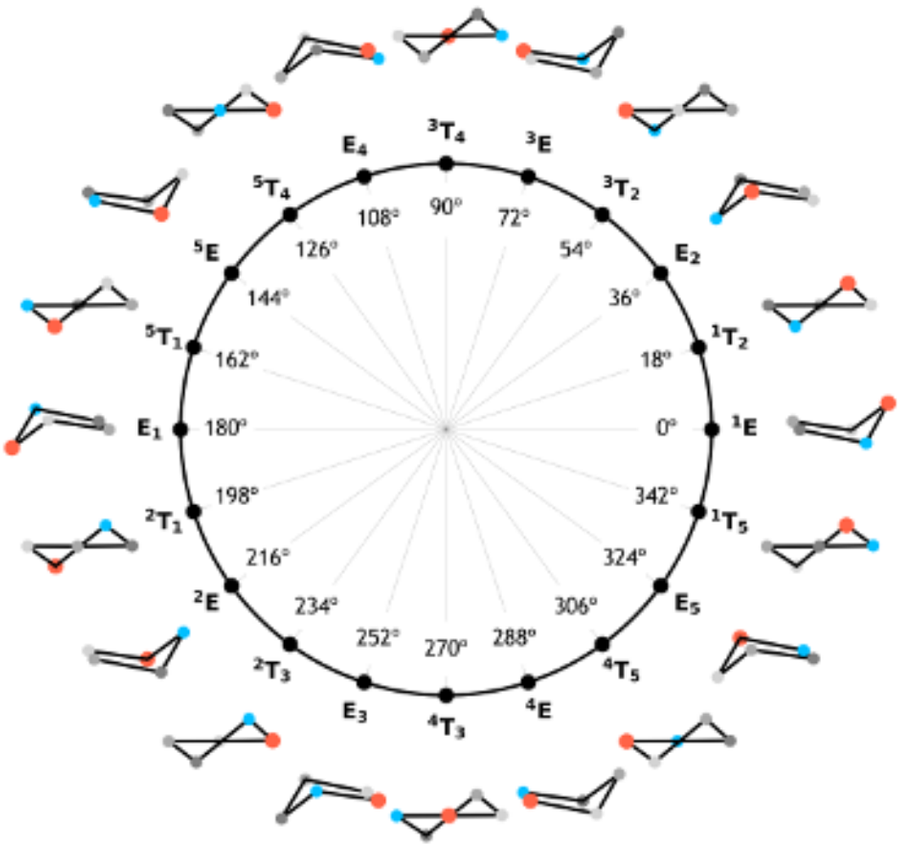

FIG. 4. Conformations of cyclopentane with representative conformers labeled; atoms 1 and 2 shown in red (larger size) and cyan, respectively. Note that to definitively establish the conformation, the numbering of the atoms should be in a clockwise direction.

projection coefficients are

$$p_{\mathrm{E}} = \langle z(\mathrm{I}), C_2 \rangle = q_2 \cos\phi_2, \tag{50a}$$
$$p_{\mathrm{T}} = \langle z(\mathrm{I}), S_2 \rangle = -q_2 \sin\phi_2, \tag{50b}$$

where $z(\mathrm{I})$ is given by the set of N equations given by Equation (C1). The percentage of each conformation is simply

$$\%\mathrm{E} = 100\,\frac{p_{\mathrm{E}}^2}{p_{\mathrm{E}}^2 + p_{\mathrm{T}}^2} = 100\cos^2\phi_2, \tag{51a}$$
$$\%\mathrm{T} = 100\,\frac{p_{\mathrm{T}}^2}{p_{\mathrm{E}}^2 + p_{\mathrm{T}}^2} = 100\sin^2\phi_2. \tag{51b}$$

To employ the projection formulas consistently, the phase should be scaled by $(\pi/2)/(\Delta\phi_2/2)$, and therefore

$$\%\mathrm{E} = 100\cos^2(5\phi_2), \tag{52a}$$
$$\%\mathrm{T} = 100\sin^2(5\phi_2). \tag{52b}$$

For cyclohexane, identical conformations appear at intervals of

$$\phi_2 = \pm\left(\phi_2^0 + \frac{2\pi}{N}k\right); \quad k = 0,\ldots,N-1. \tag{53}$$

In this case there are two amplitudes: q_2, which has an associated phase, and q_3, which is phase-independent. If $q_3 = 0$ the most notable ring structures correspond to the boat conformation (B) when $\phi_2^0 = 0$ and the skew conformation (S) when $\phi_2^0 = \pi/6$. The chair conformations (C) appear when $q_2 = 0$ and $q_3 = \pm Q$, where Q is the total amplitude. For six-membered rings the two amplitudes can be transformed into a type of 'spherical-like' coordinates (Q,ψ) given by

$$\begin{cases} Q = \sqrt{q_2^2 + q_3^2}, & Q \in [0,\infty) \\ \psi = \arccos\left(\frac{q_3}{Q}\right), & \psi \in [0,\pi] \end{cases} \tag{54}$$

and ϕ_2 as the azimuthal angle. With this representation, B and S conformations are located in the equator $(q_2 = Q, \psi = \pi/2)$

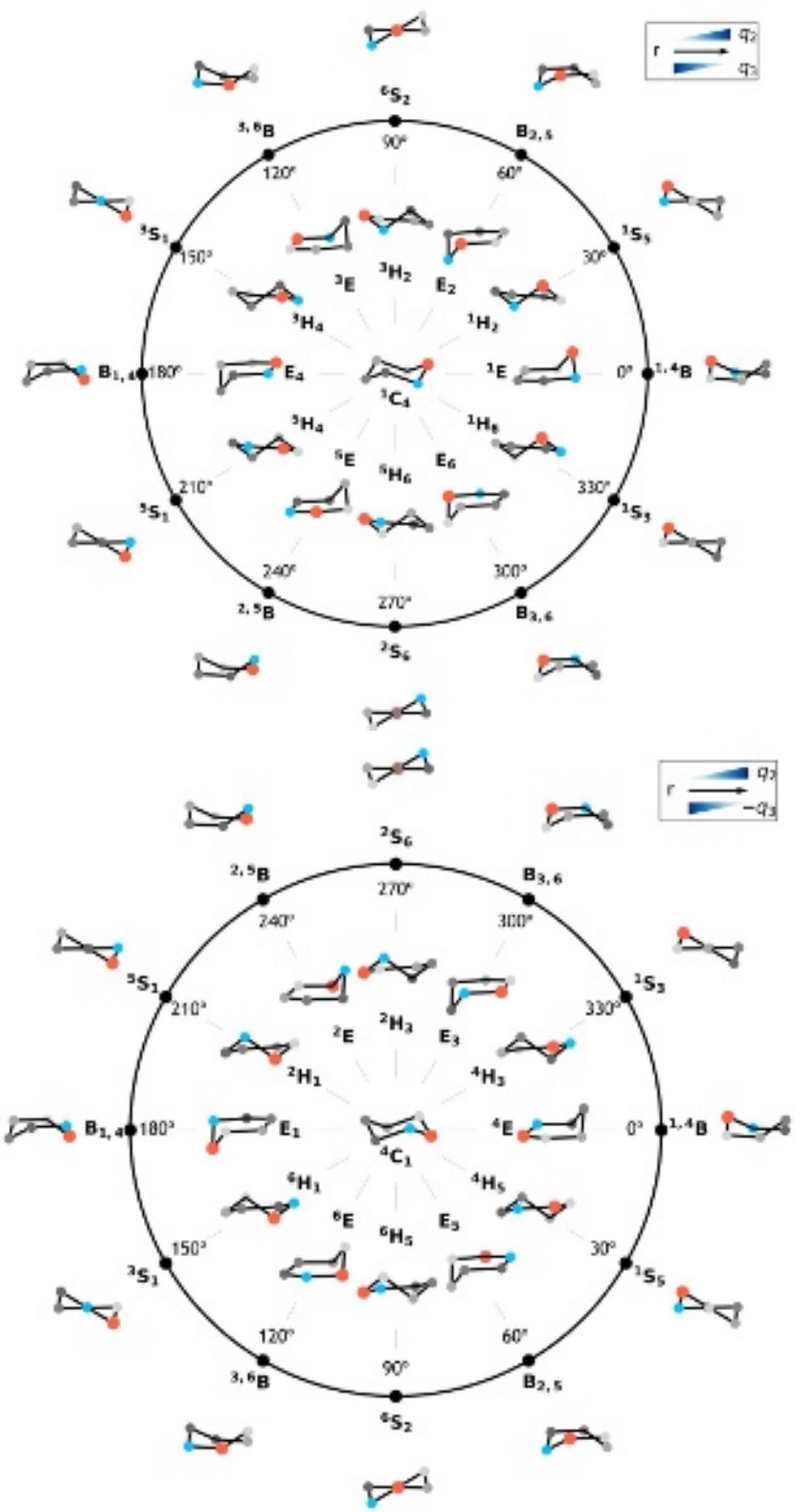

FIG. 5. Main cyclohexane conformations labeled, displaying the Northern hemisphere (top) and the Southern hemisphere (bottom); atoms 1 and 2 are colored red (larger size) and cyan, respectively. Conformations B and S are located at the equator $q_2 = Q$, while E and H conformations appear at $q_2 = \pm q_3$, and C conformation when $q_3 = \pm Q$ (plus sign for Northern and minus sign for Southern hemispheres, respectively.

and C conformations in the poles, i.e., $(q_3 = Q, \psi = 0)$ in the North Pole and $(q_3 = -Q, \psi = \pi)$ in the South Pole. Intermediate structures between the poles and the equator can be obtained with $q_2 = Q/\sqrt{2}$ and $q_3 = \pm Q/\sqrt{2}$. These correspond to $\psi = \pi/4, 3\pi/4$ and to the half-boat or envelope (E) ($\phi_2^0 = 0$) and half-chair (H) ($\phi_2^0 = \pi/6$) structures. Figure 5 illustrates these structures.

The half-boat conformation has 50% of chair and 50% of boat conformations, whereas the half-chair one has 50% of chair and 50% of skewed conformations. The percentage of chair of a given conformation I is simply

$$\%\mathrm{C} = 100 \times \left(\frac{q_3}{Q}\right)^2, \tag{55}$$

whereas the percentage of boat conformation is

$$\%\mathrm{B} \;=\; 100 \times \left(\frac{q_2}{Q}\right)^2 \cos^2(3\,\phi_2), \tag{56}$$

and the percentage of the skewed conformation is

$$\%\mathrm{S} \;=\; 100 \times \left(\frac{q_2}{Q}\right)^2 \sin^2(3\,\phi_2) \tag{57}$$

Equation (54) shows that Q is the total amplitude, that is the radius of the sphere, and ψ fixes the position along a meridian. Then for each value of (Q, ψ), the phase of Eq. (53) indicates the corresponding parallel on the sphere. The natural extension of Eq. (54) to more dimensions is the hyperspherical coordinates, which relate the amplitudes to a set of $\{Q, \psi_1, \psi_2, \ldots, \psi_{\mathrm{K}-2}\}$ given by the relation

$$\begin{cases} Q_k = \sqrt{\sum_{m=2}^{k} q_m^2}; \quad Q = Q_{\mathrm{K}} \\ \psi_1 = \arccos\left(q_3/Q_3\right) \\ \psi_2 = \arccos\left(q_4/Q_4\right) \\ \vdots \\ \psi_{\mathrm{K}-2} = \arccos\left(q_{\mathrm{K}}/Q\right), \end{cases} \tag{58}$$

where $K = M$ if N is odd and $K = M + 1$ if N is even. The inverse transformation is given by

$$\begin{cases} q_{\mathrm{K}} = Q\cos(\psi_{\mathrm{K}-2}) \\ q_{\mathrm{K}-1} = Q\sin(\psi_{\mathrm{K}-2})\cos(\psi_{\mathrm{K}-3}) \\ q_{\mathrm{K}-2} = Q\sin(\psi_{\mathrm{K}-2})\sin(\psi_{\mathrm{K}-3})\cos(\psi_{\mathrm{K}-4}) \\ \vdots \\ q_3 = Q\sin(\psi_{\mathrm{K}-2})\sin(\psi_{\mathrm{K}-3})\cdots\sin(\psi_2)\cos(\psi_1) \\ q_2 = Q\sin(\psi_{\mathrm{K}-2})\sin(\psi_{\mathrm{K}-3})\cdots\sin(\psi_2)\sin(\psi_1). \end{cases} \tag{59}$$

The total amplitude Q takes values in the range $[0, \infty)$, and each angle ψ_k takes values in the range $[0, \pi/2]$ except $\psi_{\mathrm{K}-2}$ that ranges over $[0, \pi]$ if N is even. This is because all values of q_m are positive except when N is even for which $q_{\mathrm{N}/2}$ can be negative.

These new coordinates facilitate the mapping of the conformational space, because it is straightforward to explore several phases within the same hypersphere. Table I lists the values of the hyperspherical angles for the representative conformations.

For seven-membered rings (Q, ψ) coordinates are similar as for the six-membered ring but ψ takes values in the range $[0, \pi/2]$. For each mode, $m = 2, 3$, the two basis conformations are obtained by applying Eq. (C1) at $\phi_m = \phi_m^0$ and $\phi_m = \phi_m^0 + \pi/2$ to this case, as shown in Table I. A recent and extensive discussion of the ring conformations of cycloheptane, based in the work of Bocian *et al.*[41] can be found in Ref. 42. It is also possible to represent the basis conformations of seven-membered rings by pairs (q_2, ϕ_2) and (q_3, ϕ_3) as indicated in Ref. 43.

For an eight-membered ring of indistinguishable atoms, when $q_3 = q_4 = 0$ the phases $\phi_2 = 0$ and $\phi_2 = \pi/2$ span the $m = 2$ subspace and thus constitute a basis in the linear-algebraic sense. However, the two geometries are symmetry-equivalent [both correspond to the boat-boat (BB) conformation], so they are not distinct conformers. The structure at $\phi_2 = \pi/4$ leads to a twist-boat (TB) conformation and can be regarded as the most contrasting geometry relative to BB, i.e., a representative conformation, but it is not a basis conformation in the sense of orthogonality; therefore, projection-based formulas such as Eq. (52) do not apply here. For $N = 8$ an approximate way of giving the percentage of BB of a given I conformation is

$$\%\mathrm{BB} = 100\left(\frac{q_2}{Q}\right)^2 \left(1 - \frac{\pi}{4}|\phi_2(\mathrm{TB}) - \phi_2(\mathrm{I})|\right), \tag{60}$$

where $\phi_2(\mathrm{TB})$ is given by the closest phase of a TB conformation to $\phi_2(I)$. Symmetry-equivalent structures are generated by

$$\phi_2 = \pm\left(\phi_2^0 + \frac{4\pi}{N}k\right), \qquad k = 0, \ldots, \frac{N}{2} - 1. \tag{61}$$

For $q_3 = Q$ with $q_2 = q_4 = 0$, the representative conformation at $\phi_3 = 0$ has the shape of a long-chair (L). The phases $\phi_3 = \pi/4$ and $\phi_3 = \pi/2$ generate structures that are symmetry-equivalent to $\phi_3 = 0$; the most contrasting geometry occurs at $\phi_3 = \pi/8$ and is a chair (C). The difference between L and C conformations is that L contains six atoms in the mean plane (e.g., for $\phi_3 = 0$, atom $j = 1$ is above the plane and atom $j = 5$ below it and the other six are in the mean plane), whereas C only contains four atoms in the mean plane (e.g., for $\phi_3 = \pi/8$, atoms $j = 3, 4$ are above the plane and atoms $j = 7, 8$ below it). The percentage of L of a given conformation is

$$\%\mathrm{L} = 100\left(\frac{q_3}{Q}\right)^2 \left(1 - \frac{\pi}{8}|\phi_3(\mathrm{C}) - \phi_3(\mathrm{I})|\right). \tag{62}$$

The family of symmetry-equivalent conformations is given by

$$\phi_3 = \pm\left(\phi_3^0 + \frac{2\pi}{N}k\right), \qquad k = 0, \ldots, N - 1. \tag{63}$$

Finally, for $q_4 = \pm Q$ with $q_2 = q_3 = 0$, the conformation is phase-independent and corresponds to the crown conformation (W), and the percentage of W in a conformation I is

simply

$$\%\mathrm{W} = \left(\frac{q_4}{Q}\right)^2 \times 100. \tag{64}$$

The concept of basis conformations introduced by Cremer[39] allows a systematic classification of conformations, despite the impossibility of finding an orthonormal basis for $N = 8$ with two distinguishable structures (a situation that also arises for $N = 12$ when $q_3 = Q$). In all other cases up to $N = 15$, any conformation can be classified as a combination of basis conformations in the same manner described in this section.

If symmetry is ignored, the number of calculations required to determine all conformations listed in Table I is $4N$ for $N = 5$, $2N+2$ for $N = 6$, $8N$ for $N = 7$ and $3N+2$ for $N = 8$. However, a search based solely on one amplitude different from zero may overlook important conformations, especially in rings containing heteroatoms. Therefore, we propose a preconditioned search that, in addition to phases with the initial values of ϕ_m^0 discussed above, also considers pairs with amplitudes $q_m = q_{m'} = Q/\sqrt{2}$ and all other $q_{m''} = 0$. For example, for $N = 8$, these pairs include (q_2, q_3), (q_2, q_4), and (q_3, q_4), which correspond to the hyperspherical angles (ψ_1, ψ_2) of $(\pi/4, \pi/2)$, $(\pi/2, \pi/4)$, and $(0, \pi/4)$, respectively.

The total number of calculations for an eight-membered ring molecule using the mapping described above, without accounting for any symmetry, is 26 when just one amplitude $q_m \neq 0$, plus the combinations of pairs that amount to 8×16 + 8×2 + 16×2 = 176. Thus, the overall total of calculations is 202. This search can be easily extended to other amplitudes or hyperspherical coordinates. For instance, exploring the hypersphere with $(\psi_1 = \pi/4, \psi_2 = \pi/4)$ corresponds to values of $q_2 = q_3 = Q/2$ and $q_4 = \pm Q/\sqrt{2}$. A complete exploration with steps for ϕ_2 and ϕ_3 every $\pi/4$ and $\pi/2$ radians, respectively, involves 8×16 conformations for each hemisphere. However, our findings for cyclooctane indicate that such exhaustive search was unnecessary.

Note that in many cases, applying symmetry can substantially reduce the number of calculations required. However, in this manuscript, we focus on the performance of the algorithm and its ability to locate all conformations, even if some of them are equivalent. In a forthcoming work, we will analyze the impact of symmetry on the number of conformations to be evaluated, specifically for intermediate-sized rings (from 9 to 14 members).

Finally, there is an issue related to the initial value of the total amplitude. From a practical standpoint, the algorithm performs better if the starting or reference geometry is already an optimized conformer. For the generation of a geometry with new CP coordinates, we choose the bond lengths and bond angles from the closest optimized geometry, along with the total amplitude. To identify this optimized structure, the distance between hyperspherical angles and CP phases of the two geometries is computed. The chosen optimized structure from which the geometric parameters are taken is the structure that minimizes

$$\|\mathbf{d}\| = \sqrt{\sum_{k=1}^{\mathrm{K}-2} \left(\psi_k - \psi_k^\circ\right)^2 + \sum_{m=2}^{\mathrm{M}} \left(\phi_m - \phi_m^\circ\right)^2}, \tag{65}$$

where the angles of the reference geometry are denoted with the superscript $\circ$.

III. APPLICATIONS

Electronic structure calculations, linked to RRA, were employed to find the conformations of several rings containing up to eight atoms, including cycloalkanes, five-membered heterocycles, and cycloalkenes, along with a comparison between RRA and Cremer's method. All geometries were optimized with the ωB97X-D[44] DFT method and the def2-TZVPP basis set[45] employing *Gaussian*16.[46] The RRA procedure was implemented in an in-house code; a public release is planned in the near future. The geometries of all conformers discussed in this section are available on Zenodo.[47]

A. Cycloalkanes

The first test for RRA involved the study of cycloalkanes in rings containing 5 to 8 members. At the ωB97X-D DFT level the minimum of cyclopentane is at 14.6°, which does not correspond to any representative conformation, although the structure is more similar to a twisted conformation. In this case, there are 20 equivalent conformers.

TABLE II. Cycloalkanes with their corresponding CP coordinates. The values n_{eq}/PG indicate the number of equivalent structures and the point group symmetry of each conformation, respectively. The relative energy differences between conformations, ΔE, are given in kcal mol^{-1}. All structures were optimized at the ωB97X-D/def2-TZVPP level of theory.

Molecule	CP coordinates					n_{eq} / PG	ΔE
	q_2	ϕ_2	q_3	ϕ_3	q_4		
Cyclopentane	0.406	14.6	—	—	—	20 / C_1	0.00
Cyclohexane	0.000	0.0	±0.563	—	—	2 / D_{3d}	0.00
	0.771	30.0	0.000	—	—	6 / D_2	6.30
Cycloheptane	0.525	12.9	0.643	64.3	—	14 / C_2	0.00
	1.149	0.0	0.014	180.0	—	14 / C_s	3.40
Cyclooctane	1.031	90.0	0.585	45.0	−0.343	16 / C_s	0.00
	0.000	0.0	0.000	0.0	±0.805	2 / D_{4d}	1.60
	0.721	45.0	0.815	22.5	−0.225	16 / C_2	1.80
	1.552	15.3	0.000	0.0	0.000	8 / S_4	3.30

For cyclohexane, it is well known that the conformers correspond to chair and skew structures.[48] Each skew conformer has a phase given by Eq. (53) and correspond to each of the six S structures of Figure 5.

Cycloheptane also presents two conformers in which the twist-chair (TC) is considered to be the absolute minimum.[31,49,50] However, the CP coordinates for this structure

shown in Table II indicate that the most stable conformer is a combination of TB and TC conformations. The value of $q_2 = 0.525$ Å and $q_3 = 0.643$ Å correspond to a total amplitude of $Q = 0.830$ Å . These values of q_2 and q_3 agree well with the ones of Zou *et al.*[31] which amount to 0.547 Å and 0.649 Å, respectively. The phases of $\phi_2 = \pi/14 = 12.9°$ and $\phi_3 = 5\pi/14 = 65.3°$ correspond to pure TB and TC conformations, respectively. Therefore the percentage of each of the conformations is given by the value of the amplitudes, which amounts to 40% TB and 60% TC. The other conformer, which is less stable by 3.4 kcal/mol is a B conformer.

In the case of cyclooctane, the most stable conformer (with 16 equivalent structures) is composed of approximately 70% BB, about 20% L, and 10% W. Despite the high BB contribution, the resulting structure resembles a boat-chair (BC), which is how it is described in the literature.[31,50] The minimum twist-chair-chair reported by Zou *et al.*[31] at the MP2 level was not found at the ωB97X-D level, a situation that also occurs at the B3LYP level.[50] Another minimum corresponds to the W conformer, which at the ωB97X-D level is slightly more stable than the twist-boat-chair (TBC) by 0.20 kcal/mol. The highest-energy conformer corresponds to a slightly distorted BB structure ($\phi_2 = 15.3°$) with S_4 symmetry. The pure BB structure, for which $\phi_2 = 0$, is a transition state with D_{2d} symmetry.

B. Comparison of RRA with Cremer's method

At this point, it is worthwhile to compare RRA with Cremer's method[17] (see Appendix D). Both approaches aim to generate new conformations of molecular rings while preserving structural integrity, although they differ significantly in methodology. Our algorithm systematically transforms reference coordinates into projected coordinates, maintaining bond lengths and allowing for controlled angle adjustments. In contrast, Cremer's method projects internal coordinates and constructs the ring through geometric steps, focusing the distortion of the ring on three specific angles. While it preserves the overall ring structure, Cremer's method can yield highly heterogeneous angle distributions when the reference and target conformations differ substantially, and in such cases it often fails to reconstruct the ring.

Figure 6 shows the projected ring structures obtained by Cremer's method and RRA for the reconstruction of the BB conformation, employing the crown optimized geometry from Table II as reference. For this reference, $r_j^\circ = 1.530$ Å and $\theta_j^\circ = 118.1°$ for $j = 1,\ldots,N$, with $q_4 = 0.805$ Å. In Cremer's method, the angles associated with the reconstruction of the triangle are too large, specifically angles θ_2, θ_4, and θ_7, and at $q_2 = 1.6$ Å, it is not possible to reconstruct the ring using this method. In contrast, RRA redistributes the distortion across all angles, providing a more realistic initial geometry for any value of q_2.

To compare both reconstructions quantitatively, we evaluate: (i) the root-mean square (RMS) deviation of bond angles from the reference values, $\Delta\theta_{\rm RMS}$.

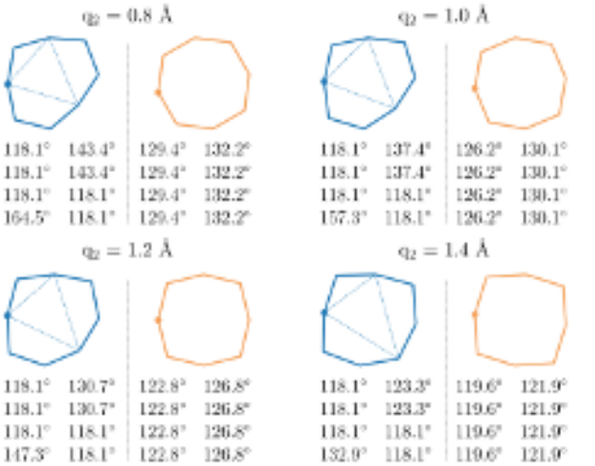

FIG. 6. Projection onto the mean plane of the resulting structures obtained by the Cremer's method (blue) and RRA (orange) after reconstructing a new conformation of cyclooctane with $q_2 > 0$, $\phi_2 = 0°$ and $q_3 = q_4 = 0$ (BB conformation) using the crown conformer as representative. Atoms are numbered clockwise starting with the dot (atom 1). The resulting eight bond angles (in degrees) are θ_1 (atoms 7-8-1, top-left), θ_2 (atoms 8-1-2, top-right),...,θ_7 (atoms 5-6-7, bottom-left), and θ_8 (atoms 6-7-8, bottom-right).

Specifically, if $\Delta\theta_j = \theta_j - \theta_j^\circ$ then

$$\Delta\theta_{\rm RMS} = \sqrt{\frac{1}{N}\sum_{j=1}^{N}(\Delta\theta_j)^2}, \tag{66}$$

and (ii) the maximum deviation

$$\Delta\theta_{\rm max} = \max_{1\le j\le N}|\Delta\theta_j|. \tag{67}$$

TABLE III. Quantitative reconstruction metrics for two cyclooctane representative conformations (BB and C) employing as reference the crown optimized geometry (see text and Figure 6). Angle deviations are relative to the reference angles $\{\theta_j^\circ\}$ in degrees.

Conformation	Q (Å)	Cremer		RRA (This work)	
		$\Delta\theta_{\rm RMS}$	$\lvert\Delta\theta\rvert_{\rm max}$	$\Delta\theta_{\rm RMS}$	$\lvert\Delta\theta\rvert_{\rm max}$
BB	0.6	23.9	51.8	14.7	15.5
	0.8	20.8	46.5	12.8	14.1
	1.0	16.9	39.2	10.3	12.0
	1.2	12.1	29.3	7.0	8.7
	1.4	5.9	14.9	2.9	3.8
	1.6	—	—	2.0	2.7
C	0.4	19.9	37.0	13.6	14.0
	0.6	13.3	23.7	9.5	10.5
	0.8	4.8	9.1	4.4	6.2
	1.0	—	—	5.6	8.1
	1.2	—	—	14.2	20.1

Table III complements Figure 6 and quantifies the differences between the RRA and Cremer algorithms. For the BB

conformation, Cremer's method fails precisely for the amplitude with the smallest RMS deviation with respect to the reference geometry. For the C conformation, both methods yield the smallest RMS at $Q = 0.8$ Å; however, Cremer's method fails when Q is increased only slightly beyond this optimum value. This combination of failures at some Q values and large deviations at others makes Cremer's approach less robust than RRA and of limited usefulness for automated sampling.

Cremer's method can be regarded as a specific case of our algorithm, and its RMS deviation is always equal to or larger than that of RRA. In fact, RRA provides the same result if, rather than minimizing across all angles, one solves the system formed by Eqs. (28), (30), and (31) while holding all angles fixed except θ_2, θ_4, and θ_7. Equivalently, this corresponds to solving the Lagrangian in Eq. (37) with large γ_j values assigned to all remaining angles, thereby concentrating the distortion on those three.

C. Heterocycles of five-membered rings

Another test was to find the conformers of all the five-membered systems described by Paoloni *et al.*,[28] which are listed in Table IV. These authors employed a different DFT method (B2PLYP-D3BJ), but the results agree very well with our calculations for the amplitude and phase of the CP coordinates. The presence of heteroatoms reduces the number of equivalent structures. For tetrahydrofuran, the minima occur when the oxygen lies on the mean plane (at ^{3}T$_4$, $\phi_2 = 18.0°$ or in its reflection across the mean plane, at ^{4}T$_3$), or when its amplitude is maximal (conformers ^{1}E and E$_1$), as shown in Figure 4. When the heteroatom is sulfur, only the twisted ^{3}T$_4$ and ^{4}T$_3$ conformations are conformers.

For 1,2-dioxolane and 1,2-dithiolane, the two conformers are located on opposite sides of the mean plane and correspond to ^{1}T$_2$ and ^{2}T$_1$ structures. The molecule 1,3-dioxolane presents a minimum close to a ^{1}E conformation, with oxygen 1 having the maximum amplitude. There are four identical conformers; one is the reflection across the mean plane with $\phi_2 = 180.4°$ and has a structure very close to E$_1$. The other two equivalent conformers are very close to the ^{3}E and E$_3$ conformations (oxygen 3 has the maximum amplitude). In the case of 1,3-dithiolane, the conformer with $\phi_2 = 97.0°$ lies between the ^{3}T$_4$ and E$_4$ conformations. Its mirror image across the mean plane lies between ^{4}T$_3$ and ^{4}E. The other two equivalent structures are at $\phi_2 = 155.0°$ and $\phi_2 = 335.0°$.

In the case of 1,3-oxathiolane, there are only two conformers (instead of the four in 1,3-dioxolane and 1,3-dithiolane) because the two heteroatoms are different, so only reflection across the mean plane is possible. The two conformers of this molecule correspond to ^{5}T$_1$ for the phase $\phi_2 = 162.0°$ and ^{1}T$_5$ for the phase $\phi_2 = 342.0°$, respectively. The agreement is also good for the chlorine-substituted molecules, yielding the same number of conformers and similar CP coordinates.

TABLE IV. Same as Table II but for different five-membered rings. The CP coordinates of Ref. 28 were recalculated to be consistent with the IUPAC atom numbering.

Molecule	This work q_2	This work ϕ_2	Ref. 28 q_2	Ref. 28 ϕ_2	n_{eq} / PG	ΔE
Tetrahydrofuran	0.370	90.0	0.378	90.0	2 / C_2	0.00
	0.367	0.0	0.376	0.0	2 / C_s	0.05 (0.03)[a]
Tetrahydrothiofene	0.433	90.0	0.44	90.0	2 / C_2	0.00
1,2-dioxolane	0.437	18.0	0.45	18.0	2 / C_2	0.00
1,3-dioxolane	0.344	0.4	0.357	356.2	4 / C_1	0.00
1,2-dithiolane	0.645	18.0	0.66	18.0	2 / C_2	0.00
1,3-dithiolane	0.512	97.0	0.519	99.5	4 / C_1	0.00
1,2-oxathiolane	0.433	159.1	0.442	154.8	2 / C_1	0.00
1,3-oxathiolane	0.413	162.0	0.423	160.7	2 / C_1	0.00
3R,5S-dichloro-1,2-dithiolane	0.634	42.0	0.645	42.4	2 / C_1	0.00
	0.528	232.4	0.529	234.8	2 / C_1	0.89 (0.68)
3S,5S-dichloro-1,2-dithiolane	0.541	51.3	0.544	53.7	2 / C_1	0.00
3S-chloro-1,2-dithiolane	0.455	103.9	0.465	97.5	1 / C_1	0.00
	0.602	352.7	0.611	351.9	1 / C_1	0.18 (0.51)
	0.654	212.2	0.668	212.1	1 / C_1	0.86 (1.28)

[a] Energies in parentheses are from Ref. 28.

D. Cycloalkenes

Table V lists several cycloalkene conformers with one or more double bonds, together with their CP coordinates and the reduced CP coordinates obtained via the algorithm described in the previous section.

The reduced coordinates are generated by renumbering the atoms as follows: in cyclopentene and every structure containing a single double bond, atoms $j = 1$ and $j = 2$ are replaced by their midpoint (now labeled as $j' = 1$), and each remaining atom is renumbered according to $j' = j - 1$. In the case of 1,3-cycloheptadiene, the new numbering is such that $j' = 1$ for the midpoint of original atoms $j = 1, 2$, $j' = 2$ for the midpoint of $j = 3, 4$, and $j' = j - 2$ for all other atoms, as shown in Figure 7.

Cyclopentene exhibits two envelope-type E$_4$ and ^{4}E conformations in which the double bond is coplanar with the two adjacent carbon atoms, while carbon four lies out of the plane, as shown in Figure 4. This geometry corresponds to that reported by Leong et al. at the MP2/6-31G* level.[38] From the standpoint of ring deformation, it behaves like cyclobutane [see Figure 7a)]. A similar situation occurs for 1,3-cyclohexadiene, for which the ring puckering is restricted to a single amplitude, with no additional deformation possibilities. Shishkin[51] indicated that 1,3-cyclohexadiene presents two equivalent conformers with C_2 symmetry with a structure which is between chair and half-chair, but the values of the amplitude with $q_2 > |q_3|$ reveal that one conformation is between skew ^{2}S$_6$ and half-chair ^{5}H$_6$ and other between ^{6}S$_2$ and ^{6}H$_5$.

TABLE V. Same as Table II but for cycloalkenes. In bold the reduced CP coordinates.

Molecule	CP coordinates					n_{eq} / PG	ΔE
	q_2	ϕ_2	q_3	ϕ_3	q_4		
Cyclopentene	0.211/**-0.205**	108.0	—	—	—	2 / C_s	0.00
Cyclohexene	0.377/**0.480**	30.0/**90.0**	−0.307	—	—	2 / C_2	0.00
	0.622/**0.574**	120.0/**180.0**	0.000	—	—	2 / C_s	5.53
1,3-cyclohexadiene	0.359/**-0.365**	90.0	−0.165	—	—	2 / C_2	0.00
Cycloheptene	0.303/**0.067**	128.6/**180.0**	0.627/**-0.658**	102.9	—	2 / C_s	0.00
	0.843/**0.889**	38.6/**90.0**	0.357/**0.000**	192.9	—	2 / C_2	1.15
	0.884/**0.888**	94.2/**142.1**	0.300/**0.000**	226.8	—	4 / C_1	3.03
	1.083/**0.957**	128.6/**180.0**	0.005/**-0.215**	282.8	—	2 / C_s	4.51
1,3-cycloheptadiene	0.397/**0.533**	25.7/**108.0**	0.380	128.6	—	2 / C_s	0.00
	0.932/**0.804**	115.7/**198.0**	0.145	218.6	—	2 / C_2	2.07
1,4-cycloheptadiene	0.672/**0.652**	16.4/**84.8**	0.315	165.2	—	4 / C_1	0.00
	0.473/**0.516**	64.3/**126.0**	0.303	141.4	—	2 / C_2	0.05
Cyclooctene	0.875/**0.687**	107.1/**134.8**	0.685/**0.787**	148.7/**213.3**	0.287	4 / C_1	0.00
	1.342/**1.310**	4.3/**52.0**	0.269/**0.118**	181.9/**31.7**	−0.155	4 / C_1	1.88
	0.847/**0.668**	108.1/**155.0**	0.355/**0.720**	47.8/**114.8**	−0.514	4 / C_1	3.38
	0.386/**0.526**	38.5/**50.1**	0.873/**0.775**	126.0/**190.9**	0.093	4 / C_1	6.19
	0.248/**0.150**	90.5/**97.1**	0.422/**0.446**	107.6/**158.5**	−0.132	4 / C_1	56.07
1,3-cyclooctadiene	0.821/**0.314**	135.0/**210.0**	0.493/**-0.821**	67.5	−0.408	2 / C_2	0.00
	1.171/**1.089**	94.2/**162.1**	0.382/**-0.178**	168.2	0.050	4 / C_1	0.45
1,4-cyclooctadiene	1.228/**1.117**	82.5/**143.4**	0.345/**0.064**	190.2	-0.042	4 / C_1	0.00
	0.550/**0.198**	0.0/**59.9**	0.784/**0.829**	270.0	0.185	2 / C_s	0.43
	1.170/**1.062**	22.3/**81.9**	0.121/**0.111**	180.0	−0.315	4 / C_1	2.21
1,5-cyclooctadiene	1.182/**1.046**	100.0/**139.1**	0.000/**0.000**	0.0	-0.290	4 / C_2	0.00
	0.819/**0.661**	135.0/**180.0**	0.559/**0.519**	292.5	0.000	4 / C_s	2.00
	0.000/**0.000**	0.0/**0.0**	0.883/**0.834**	292.5	0.000	2 / C_{2h}	2.35

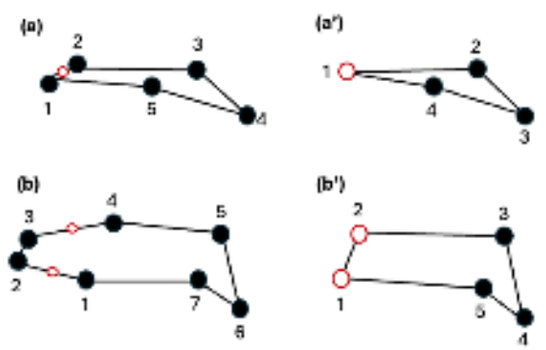

FIG. 7. Numbered ring structures of the lowest-energy conformers of (a) cyclopentane and (b) 1,3-cycloheptadiene. Midpoint of the double bonds are indicated by a hollow-red circle. Rings (a') and (b') correspond to the structures retained to compute the reduced CP coordinates.

The systems of Table V which behave as cyclopentane from the point of view of deformation are cyclohexene, 1,3-cycloheptadiene,[52,53] and 1,4-cycloheptadiene.[52,53] Cyclohexene presents two different conformers, the most stable is a conformation close to a half-chair and the other is a boat ^{3,6}B conformation in agreement with the results of Jensen and Bushweller.[54] In the case of 1,3-cycloheptadiene, the most stable conformer with C_s symmetry has CP reduced coordinates that correspond to a E_4 conformation [see Figure 7b)], whereas the other conformer with conformation $^2T_1$ and C_2 symmetry, is less stable than the former one by 2.07 kcal/mol. Saebø and Boggs[52] identified two conformers of 1,4-cycloheptadiene corresponding to the twist and envelope conformations, with the former being significantly more stable than the latter (e.g. by 10.2 kcal/mol). At the ωB97X-D level the envelope conformer vanished, leaving one twist conformer with C_2 symmetry and a $^5T_4$ conformation. The global minimum, however, is a conformer close to the $^3T_4$ conformation in reduced CP coordinates. This structure was described in Ref. 53 as 'biplanar', although our calculations indicate that the conformer exhibits a slightly twisted structure.

Molecules such as cycloheptene and 1,3-, 1,4-, and 1,5-cyclooctadiene are considered 'pseudo-six-membered' rings due to the stiffness of their double bonds. As a result, they can be described using reduced CP coordinates associated with six-membered rings. The most stable conformer of cycloheptene is a chair conformation,[38,53,55] followed by a conformer with a skew $^6S_2$ conformation. At 3.03 kcal/mol above the global minimum, there is a conformer with a shape close to the $^3S_1$ conformation. The highest-energy conformer is near

the ^{1,4}B conformation.

For cyclooctadienes, the position of the second double bond influences both the stability and the number of conformers. In the case of 1,3-cyclooctadiene, two conformers with similar energies have been reported in the literature.[56,57] The most stable conformer has reduced CP coordinates close to a chair conformation [e.g., 87% as calculated using Eq. (55)], while the other conformer is close to a skew conformation. This trend is reversed in 1,4-cyclooctadiene, which also exhibits an additional conformer with a near-skew conformation. Figure 8 displays the three conformers of 1,5-cyclooctadiene.[58,59] The most stable conformer, characterized by $q_2 \gg q_4$ and $q_3 = 0$, closely resembles a twist-boat (TB) structure. According to Table I, a pure TB form has $q_3 = q_4 = 0$ and $\phi_2 = 90°$, which in the reduced notation places it between ^{3,6}B and ^{3}S$_1$. The second most stable conformer adopts a biplanar (envelope-type) geometry, corresponding to the E$_4$ reduced structure. This biplanar conformer is 0.35 kcal/mol more stable than the chair form shown in Figure 8c.

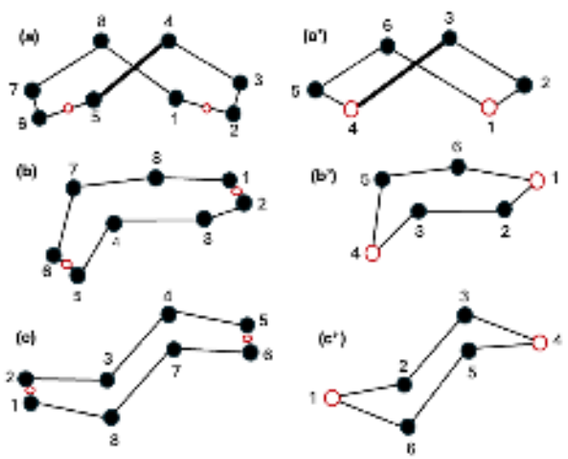

FIG. 8. Numbered ring structures of the three conformers of 1,5-cyclooctane. Conformer (a), (b) and (c) correspond to the (a') skew, (b') envelope, and (c') chair conformations using the midpoint (hollow-red circle in the left-side structures) and reduced CP coordinates procedure described in the text.

For the case of cyclooctene, Neuenschwander and Hermans[60] described four different conformers using the CCSD(T)/6-31G(d,p)//B3LYP/6-31G(d,p) level of theory. The four lowest-energy structures indicated in Table V correspond to those described in their article, maintaining the same energy ordering and relative energy values similar to theirs. In addition, we have found a conformer with a considerably higher energy, lying 56.1 kcal/mol above the most stable one, which had not been previously reported in the literature. This conformation is quite flat with atom 5 pointing to the inner part of the ring. From the point of view of thermochemistry, at room temperature and well above it, the contribution of this structure can be neglected.

Here, we have applied the midpoint reduction and reduced CP coordinates to carbon-carbon double bonds, but the same strategy extends unchanged to double bonds containing heteroatoms. The approach can, in principle, be generalized to fused rings; in that case, however, the method must enforce shared-edge constraints (e.g., on dihedrals and projected angles) to ensure that local distortions remain compatible with global ring closure across multiple cycles. A detailed treatment of fused systems falls beyond the present scope and is left for future work.

E. Heterocycles of six- to eight-membered rings

Finally, we test the method on a few molecules containing heteroatoms (oxygen in these examples) in six- to eight-membered rings. The conformations of 1,3-dioxane are those typical of six-membered rings. The most stable is the chair conformer ^{2}C$_5$, followed by two skewed conformers ^{3}S$_1$ and ^{1}S$_5$ (see Table VI), in agreement with Ref. 61. Note that conformer ^{3}S$_1$ has the same energy as ^{1}S$_3$, and conformer ^{1}S$_5$ has the same energy as ^{6}S$_2$, ^{5}S$_1$, and ^{2}S$_6$.

TABLE VI. Same as Table II but for six- to eight-membered heterocycles. The major component of the conformer is indicated in the Cf. column.

#[a]	Cf.	CP coordinates q_2	ϕ_2	q_3	ϕ_3	q_4	n_{eq} / PG	ΔE
1	^{2}C$_5$	0.011	60.0	0.546	—	—	2 / C_s	0.00
	^{3}S$_1$	0.751	150.0	0.000	—	—	2 / C_2	5.54 (4.98)[b]
	^{1}S$_5$	0.721	30.0	0.001	—	—	4 / C_1	6.02 (6.36)
2	TC$_7$	0.536	12.7	0.633	64.1	—	4 / C_1	0.00
	TC$_3$	0.502	66.1	0.638	322.5	—	4 / C_1	0.56 (0.77)[c]
	TC$_5$	0.457	225.7	0.654	14.4	—	4 / C_1	1.06 (1.62)
	TC$_1$	0.492	270.0	0.630	270.0	—	2 / C_2	1.47 (2.49)
	TB$_5$	1.150	22.0	0.028	256.1	—	4 / C_1	3.32 (2.95)
	TB$_1$	1.117	90.0	0.015	270.0	—	2 / C_2	4.71 (5.52)
3	^{5}C	0.458	128.3	0.637	101.7	—	2 / C_1	0.00
	^{6}TB	1.127	117.7	0.037	216.8	—	2 / C_1	3.00 (2.25)[d]
	TB$_5$	0.838	42.7	0.385	192.5	—	2 / C_1	5.10 (5.33)
	TC$_7$	0.567	196.0	0.650	241.8	—	2 / C_1	6.22 (4.78)
	^{3}TC	0.552	242.5	0.643	143.3	—	2 / C_1	6.60 (5.28)
4	^{3}BC	1.027	180.2	0.574	88.1	−0.329	4 / C_1	0.00 (0.4)[e]
	^{1}BC	1.014	0.0	0.569	0.0	−0.363	2 / C_s	0.45 (0.0)
	^{4}BC	1.001	86.5	0.595	314.6	0.338	4 / C_1	0.88 (1.1)
	W	0.237	0.0	0.011	0.0	0.792	2 / C_s	1.11 (0.9)
	^{4}TBC	0.723	48.4	0.788	22.2	−0.236	4 / C_1	1.27 (–)
	^{6}TBC	0.756	223.0	0.796	112.8	0.224	4 / C_1	1.97 (–)
	^{8}TBC	0.684	49.4	0.822	202.0	−0.236	4 / C_1	2.91 (–)
	^{1}BB	1.510	0.0	0.025	180.0	−0.012	2 / C_s	3.04 (3.8)
	^{5}BC	0.946	0.0	0.628	180.0	−0.354	2 / C_s	3.33 (0.9)
	^{2}TBC	0.691	225.0	0.804	293.3	0.215	4 / C_1	5.17 (–)

[a] **1**: 1,3-dioxane; **2**: oxepane; **3**: ε-capralactone; **4**: oxocane
[b] From Ref. 61.
[c] From Ref. 62.
[d] From Ref. 43.
[e] From Ref. 63.

The first four conformers of oxepane are closely related to the most stable conformer of cycloheptane, namely the TC/TB character is about 60/40%. The presence of a heteroatom

makes several of these structures distinguishable, whereas in cycloheptane there are 14 indistinguishable structures.

In the ideal TC conformation, five atoms lie in a single plane (though not the mean plane), while the remaining two atoms form the chair ends. Here we adopt a nomenclature similar to that of Jahn *et al.*[43]. For example, in the numbering sequence {1-2(e)-3-4-5(e)-6-7}, atoms 1 and 5 are the chair ends (e). The conformation is identified by the central atom of the three atoms between the two ends; in this case, that atom is 7. The molecule is rotated such that the left chair-end atom lies above the mean plane. The conformer is denoted ^{7}TC (TC^{7+} in Ref. 43) or TC_7 (TC^{7-} in Ref. 43), depending on whether atom 7 lies on the front (number as superscript) or back (number as subscript) side in the chosen view, respectively (see Figure 9). These two structures are enantiomers; in this notation, switching only the sign gives the mirror-related conformer. Note that the ring atoms are numbered clockwise and that atom 1 is oxygen. For TB conformations, the leading atom is the one through which the C_2 axis passes in the symmetric case (for instance, the oxygen atom in the TB_1 conformation in Figure 9), and the next atom in the numbering determines the sign, i.e., positive if it lies above the mean plane and negative otherwise.

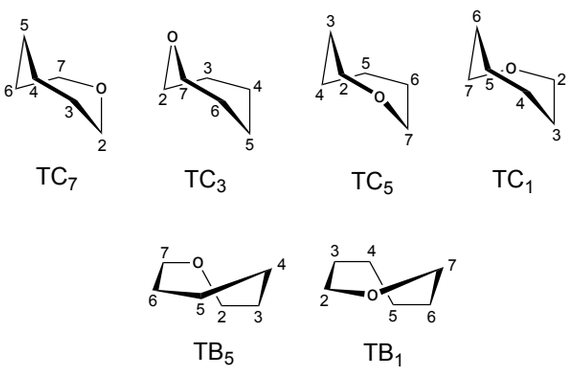

FIG. 9. Numbered ring structures of the five oxepane conformers. The structures correspond to the CP coordinates reported in Table VI. Where conformations are mixed, the label reflects only the leading conformation.

The oxepane conformers located in this work coincide with those reported in Refs. 62 and 64, including their energetic ordering. The most stable oxepane conformer is sketched in Figure 9 and resembles a TC_7 conformation. The corresponding pair (ϕ_2, ϕ_3) has phases (12.7, 64.1). Three additional structures are isoenergetic with this minimum, namely ^{7}TC, TC_2, and ^{2}TC, which correspond to the phase pairs (192.7, 244.1), (167.3, 115.9), and (347.3, 295.9), respectively. Conformers ^{7}TC and TC_2 are indistinguishable, as are TC_7 and ^{2}TC. All four isoenergetic structures were located by the RRA algorithm.

The next three conformers on the energy scale also have predominantly TC character and are labeled TC_3, TC_5, and TC_1. The first two each have three additional isoenergetic structures, as in the case of TC_7, whereas TC_1 has only its enantiomer ^{1}TC because these structures exhibit C_2 symmetry. Similar considerations apply to the less stable TB structures. Thus, TB_5 has three additional isoenergetic structures, namely ^{5}TB, TB_2, and ^{2}TB, whereas TB_1 has only the enantiomer ^{1}TB.

Another seven-membered ring molecule is ε-caprolactone. In this case, the symmetry is lower than in oxepane due to the presence of a ketone group. As a result, each conformer has an enantiomer obtained by reflection through the mean plane, but there are no additional isoenergetic conformers. This system has been studied previously by Jahn *et al.*[43] and by Groenewald and Dillen.[55] The RRA algorithm finds the same conformers as those reported in these studies, and the CP coordinates are nearly identical to those given in Ref. 43 (see Table VI). The energetic ordering agrees for the two most stable conformers but differs for the remaining three. Given the close similarity of the geometries, this discrepancy is most likely due to differences in the electronic structure methods; Ref. 43 is expected to be more accurate because it includes coupled-cluster calculations.

For oxocane, as for cyclooctane, the three most stable structures are BC conformers. They are combinations of BB and long-chair conformations and are therefore characterized by a large value of q_2 and with $q_3 \approx q_2/2$; moreover, ϕ_2 should be 0 or a multiple of 90°. On the other hand, ϕ_3 should be 0 or a multiple of 45°, as indicated by Eqs. (61) and (63). The most stable structure of oxocane is ^{3}BC, and it is shown in Figure 10 (the label indicates the number of the end atom of the boat, and superscript or subscript indicates if the end atom points up or down, respectively).

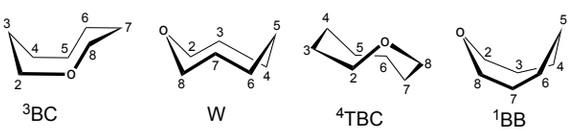

FIG. 10. Numbered ring structures of the most stable conformer of each type in oxocane. The structures correspond to the CP coordinates reported in Table VI. Where conformations are mixed, the label reflects only the leading conformation.

Yavari *et al.*[63] performed semiempirical calculations and found that the absolute minimum is ^{1}BC (which exhibits C_s symmetry); in our case, this conformer is the second-lowest minimum. However, NMR experiments and the molecular mechanics calculations of Meyer *et al.*[65] showed that ^{3}BC is likely the absolute minimum, in agreement with our calculations. Conformer ^{3}BC has three additional isoenergetic structures: ^{7}BC, BC_7, and BC_3. The semiempirical calculations of Ref. 63 do not report any TBC structure. These structures correspond to amplitudes in which $q_2 \approx q_3 > q_4$ and phases given by Eqs. (61) and (63) for which $\phi_2^0 \approx 45°$ and $\phi_3^0 \approx 22.5°$. However, the molecular mechanics calculations of Meyer *et al.*[65] correctly describe the four distinct types of TBC conformations that can occur in this molecule. Thus, their reported energies for ^{4}TBC (depicted in Figure 10), ^{6}TBC, ^{8}TBC, and ^{2}TBC are 1.10, 2.63, 3.94 and 4.86 kcal/mol, which is exactly the energy ordering reported in this work. The RRA algorithm

located all sixteen TBC conformers, which are indistinguishable in cyclooctane but form isoenergetic families of four in oxocane.

The workflow presented in the above sections can be fully automated. Starting from an input geometry, substituents are temporarily removed and the bare ring is reconstructed by our algorithm from a specified set of CP coordinates (or from a reduced set when double bonds are present). Substituents are then repositioned using the local plane-bisector scheme described above, and the full structure is subjected to electronic-structure optimization. This procedure is iterated over multiple puckering specifications to explore distinct minima. To precondition the search and improve coverage of the conformational space, hyperspherical coordinates are used to map the CP amplitudes systematically, while phases are sampled. This approach supports the efficient generation of chemically reasonable starting geometries and the systematic identification of new conformers.

IV. CONCLUSIONS

We introduced RRA, a general framework for constructing and searching conformations resulting from ring puckering directly in CP coordinates. It features accurate forward and inverse relations to Cartesian coordinates, along with a two-stage reconstruction that preserves bond lengths and distributes angular distortions throughout the ring. This approach yields chemically reasonable starting geometries for electronic structure optimization, avoiding ring opening and unrealistic angles.

The method extends naturally to rings containing rigid (multiple) bonds via ring-reduction scheme through reduced CP coordinates that lower the puckering dimensionality and incorporate local stiffness through adjustable parameters. Full structures and substituent positions can be recovered unambiguously from the reference structures.

A preconditioned exploration of conformational (puckering) space is formulated using hyperspherical coordinates over CP amplitudes. We have analyzed the concept of basis conformations introduced by Cremer[39] in 1980 across ring sizes ($N = 5-8$) providing a systematic method for classifying ring structures while facilitating an efficient search over phases and mixed-mode amplitudes. The procedure of temporarily removing substituents, reconstructing the ring from CP coordinates, repositioning substituents, and optimizing the electronic structure can be easily automated with minimal user intervention.

Applications to saturated and unsaturated rings reveal the robustness and versatility of the algorithm, accurately reproducing known conformers and equivalent structures.

ACKNOWLEDGMENTS

The authors thank Prof. E. Martínez-Núñez and Dr. Fabián Suárez-Lestón for helpful suggestions on the manuscript. A.F.-R. thanks Consellería de Educación, Ciencia, Universidades e Formación Profesional for finantial support (Centro singular de Investigación de Galicia, acreditation 2023-2027, ED431G 2023/03 and the European Regional Development Fund (ERDF), and Grupo de Referencia Competititva, ED431C 2025/06), and A. L.-S for a PhD fellowship. We also thank the Galician Supercomputing Center (CESGA) for providing access to their computing facilities.

AUTOR DECLARATIONS

Conflict of interest

The authors have no conflicts to disclose.

Author contributions

A.F.-R. and A.L.-S. designed the method. A.L.-S. implemented the algorithm, performed the electronic-structure calculations, and drafted the initial manuscript. A.F.-R. prepared the final version of the manuscript, and both authors revised it.

DATA AVAILABILITY

The data are available on Zenodo repository publicly accessible at `https://doi.org/10.5281/zenodo.17831714`

Appendix A: Summary of symbols (Notation)

For readability, we summarize the main symbols used throughout the manuscript. The symbols described below also apply to the reference geometry but with a $\circ$ as superscript.

- N: number of atoms in the ring.
- j: atom index in the ring, $j = 1,\ldots,N$, with cyclic indexing (e.g., $j-1 \equiv N$ for $j = 1$ and $j+1 \equiv 1$ for $j = N$).
- $\{\mathbf{R}_j\}_{j=1}^{N}$: Cartesian position vectors of the ring atoms.
- $\{z_j\}_{j=1}^{N}$: signed out-of-plane coordinates relative to the mean plane.
- r_j: bond length between atoms j and $j-1$.
- $\mathbf{r}_j$: bond vector used in construction (with length r_j).
- θ_j: bond angle at atom j (formed by bonds $(j-1, j)$ and $(j, j+1)$).
- φ_j: dihedral (torsion) angle associated with consecutive bonds around the ring.

- $\{r_j, \theta_j, \varphi_j\}$: geometry of the ring in internal coordinates. The geometry is fully determined (Z-matrix) even if $r_1, \theta_1, \theta_2, \varphi_1, \varphi_2, \varphi_3$ are not specified.
- s_j: projected bond length of r_j in the mean plane.
- α_j: projected bond angle of θ_j in the mean plane.
- $\{s_j, \alpha_j, z_j\}$: geometry of the ring in projected bond lengths and bond angles plus out-of-plane Cartesian coordinates.
- $\boldsymbol{\alpha} = (\alpha_3 \ldots, \alpha_N)$: vector of in-plane angles used as optimization variables.
- $\boldsymbol{\theta} = (\theta_3 \ldots, \theta_N)$: vector of 3D angles used as optimization variables.
- m: puckering-mode index in the CP coordinates.
- $\{q_m, \phi_m\}$: CP amplitudes and phases.
- Q: total puckering amplitude, defined from the set $\{q_m\}$.
- $\{\psi_k\}$: hyperspherical angles.
- $\{Q, \psi_k, \phi_m\}$: CP coordinates in hyperspherical coordinates.

Appendix B: Amplitude and bond angles in cyclobutane

The effect of the amplitude of distortion over the bond angles can be easily illustrated with cyclobutane, whose puckering is described solely by the amplitude q_2. In a planar configuration, the bond angles of this molecule are all 90°. When the square is folded by an angle φ with respect to the xy plane, the bond angle θ between the atoms involved in the folding also changes. The relationship between these two quantities is given by:

$$\theta = \arccos\left[\sin^2\left(\frac{\varphi}{2}\right)\right] \tag{B1}$$

and shown in Figure 11.

It is clear that there is a variation of θ with the folding. However, Figure 11 also shows that if the folding is not very large the variation of the angle is small. For cyclobutane, the single puckering amplitude is related to the folding angle by Eq. (6), which for the cyclobutane is

$$q_2 = \frac{r}{\sqrt{2}} \sin\varphi, \tag{B2}$$

considering that the distance between bonded atoms is r. For small amplitudes $\sin\varphi \approx \varphi$, and eq B2 is simply

$$q_2 = \frac{r}{\sqrt{2}} \varphi. \tag{B3}$$

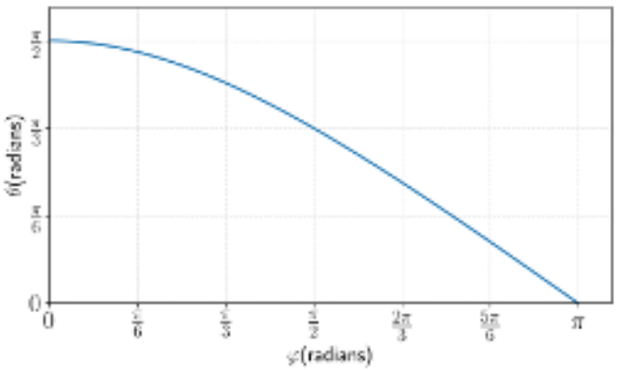

FIG. 11. Variation of the bond angle θ with the folding angle φ following Equation (B1).

Appendix C: Basis conformations

The concept of basis conformations introduced by Cremer[39] can be formulated in a rigorous mathematical way. For cyclopentane, the cosine/sine components C_2 and S_2 (envelope-like and twist-like families) serve as basis conformations in that they are orthogonal with respect to the geometric (discrete inner-product) metric. For each mode with amplitude $q_m \neq 0$ (with all other amplitudes set to zero), Eq. (4) can be written as

$$\begin{aligned} z_j &= \sqrt{\frac{2}{N}}\, q_m \cos(\phi_m + \varphi_j) \\ &= q_m \Big[C_m(j) \cos\phi_m \; - \; S_m(j) \sin\phi_m \Big], \end{aligned} \tag{C1}$$

where

$$C_m(j) = \sqrt{\frac{2}{N}} \cos\varphi_j, \tag{C2a}$$

$$S_m(j) = \sqrt{\frac{2}{N}} \sin\varphi_j, \tag{C2b}$$

and the angle $\varphi_j = (2\pi m(j-1))/N$. Thus, for $N = 5$, taking $m = 2$ and atom $j = 1$: when $\phi_2 = 0$, z_1 reaches its maximum amplitude, whereas for $\phi_2 = \pi/5$, atom $j = 2$ reaches its minimum amplitude. Continuing this way, each of the five atoms attains its maximum and minimum in turn, for a total of 10 envelope structures. The conformations orthogonal to the E structures occur when the cosine coefficient vanishes and the sine term is extremal, i.e., upon shifting the phase by $\pi/2$. Thus, for $\phi_2 = \pi/2$, atom $j = 1$ lies in the mean plane, and for $\phi_2 = 7\pi/10$, atom $j = 2$ does. In this way, the T conformations are generated and can be considered orthogonal to the E ones, and the discrete inner-product

$$\langle C_2, S_2 \rangle = \sum_{j=1}^{5} C_2(j)\, S_2(j) = 0 \tag{C3}$$

vanishes by orthogonality of the basis functions. Notice also that $\langle C_2, C_2 \rangle = \langle S_2, S_2 \rangle = 1$.

Appendix D: Cremer's method for ring reconstruction

Cremer proposed to begin with the set $\{r_j^o, \theta_j^o, z_j\}$, which is transformed into the set $\{s_j^o, \alpha_j^o, z_j\}$ following Eqs. (22) to (24). Figure 12 illustrates the steps to reconstruct a new conformation of cyclooctane with new Cremer-Pople coordinates (CP coordinates) following this method.

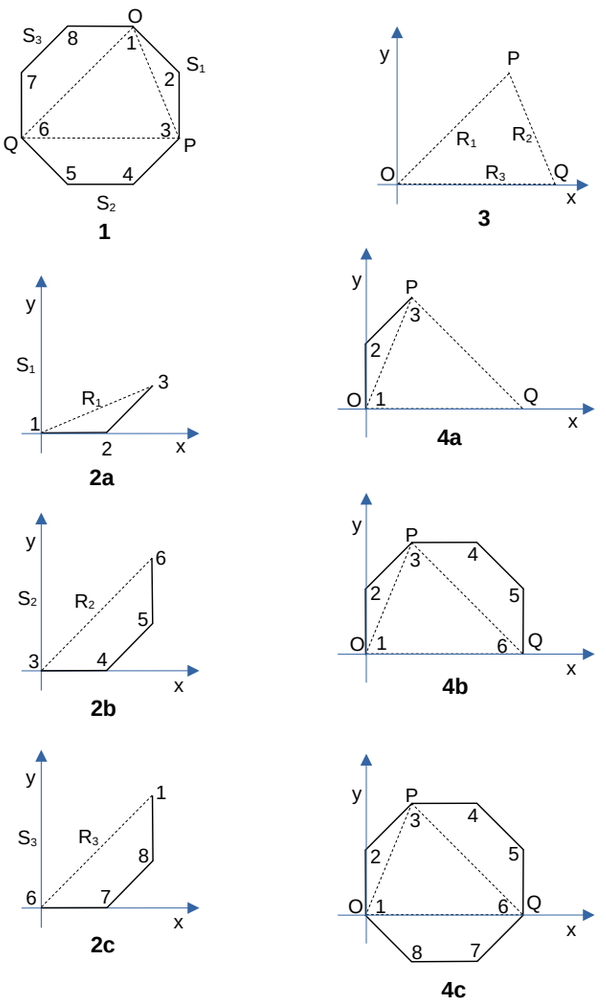

FIG. 12. Steps in the construction of a geometry with specific CP coordinates employing the method of Cremer. In this reconstruction the initial and final conformations have the same CP coordinates.

The first step is to divide the hypothetical polygon of the molecular ring into three sections S_p, with $p = 1, 2, 3$, chosen to be as similar as possible [Figure 12(1)]. The second step is to take each of these three parts and project the reference distances and angles $\{r_{j_p}^o, \theta_{j_p}^o\}$ using the z_j values. The resulting in-plane parts S_p are then joined to close the polygons by segments R_p, as shown in Figures 12(2a–c).

In the third step, the segments R_p are joined to form a triangle [Figure 12(3)], and in the fourth step, the three sections are added to the triangle [Figure 12(4a−c)], forming a closed in-plane ring. Finally, the z_j values are incorporated into the ring, recovering all the r_j^o and part of the θ_j^o angles, specifically $N-3$ of them.

[1]E. L. Eliel, N. L. Allinger, S. J. Angyal, and G. A. Morrison, *Conformational Analysis* (Interscinece Publishers (Wiley & Sons. Inc.) New York, 1965).
[2]A. Mazzanti and D. Casarini, WIREs Comput. Mol. Sci. **2**, 613 (2012).
[3]G. J. Davies, A. Planas, and C. Rovira, Acc. Chem. Res. **45**, 308 (2012).
[4]J. Zheng and D. G. Truhlar, J. Chem. Theory Comput. **9**, 1356 (2013).
[5]V. Dragojlovic, ChemTexts **1**, 14 (2015).
[6]P. Pracht, F. Bohle, and S. Grimme, Phys. Chem. Chem. Phys. **22**, 7169 (2020).
[7]D. Ferro-Costas, I. Mosquera-Lois, and A. Fernández-Ramos, J. Cheminform. **13**, 100 (2021).
[8]E. Dzib and G. Merino, WIREs Comput. Mol. Sci. **12**, e1583 (2022).
[9]P. Pracht, S. Grimme, C. Bannwarth, F. Bohle, S. Ehlert, G. Feldmann, J. Gorges, M. Müller, T. Neudecker, C. Plett, S. Spicher, P. Steinbach, P. A. Wesolowski, and F. Zeller, J. Chem. Phys. **160** (2024).
[10]J. E. Kilpatrick, K. S. Pitzer, and R. Spitzer, J. Am. Chem. Soc. **69**, 2483 (1947).
[11]H. L. Strauss and H. M. Pickett, J. Am. Chem. Soc. **92**, 7281 (1970).
[12]H. M. Pickett and H. L. Strauss, J. Chem. Phys. **55**, 324 (1971).
[13]D. Cremer and J. A. Pople, J. Am. Chem. Soc. **97**, 1354 (1975).
[14]H. Essén and D. Cremer, Acta Cryst. **B40**, 418 (1984).
[15]G. H. Petit, J. Dillen, and H. J. Geise, Acta Cryst. **B39**, 648 (1983).
[16]D. Cremer, Acta Cryst. **40**, 498 (1984).
[17]D. Cremer, J. Phys. Chem. **94**, 5502 (1990).
[18]H. Geise, C. Altona, and C. Romers, Tetrahedron Lett. **8**, 1383 (1967).
[19]C. Altona, H. t. Geise, and C. Romers, Tetrahedron **24**, 13 (1968).
[20]C. t. Altona and M. Sundaralingam, J. Am. Chem. Soc. **94**, 8205 (1972).
[21]J. C. A. Boeyens, Acta Crystallogr. B **45**, 577 (1989).
[22]J. C. A. Boeyens and D. G. Evans, Acta Cryst. **B45**, 577 (1989).
[23]D. G. Evans and J. C. A. Boeyens, Acta Cryst. **B45**, 581 (1989).
[24]N. S. Zefirov, V. A. Palyulin, and E. E. Dashevskaya, J. Phys. Org. Chem. **3**, 147 (1990).
[25]Y. Zotov, A, V. A. Palyulin, and N. S. Zefirov, J. Chem. Inf. Comput. Sci. **37**, 766 (1997).
[26]A. L. Esteban, E. Ruiz, E. Diez, and J. San-Fabian, J. Phys. Chem. **98**, 10440 (1994).
[27]S. Alonso-Gil, J. Comput. Chem. **42**, 1526 (2021).
[28]L. Paoloni, S. Rampino, and V. Barone, J. Chem. Theory Comput. **15**, 4280 (2019).
[29]E. Charvati and H. Sun, J. Phys. Chem. A **127**, 2646 (2023).
[30]L. Chan, G. R. Hutchison, and G. M. Morris, J. Chem. Inf. Model. **61**, 743 (2021).
[31]W. Zou, Y. Tao, and E. Kraka, J. Chem. Phys. **152**, 154107 (2020).
[32]H. B. Curry, Quart. Appl. Math. **2**, 258 (1944).
[33]S. Ruder, arXiv: arXiv:1609.04747 (2023).
[34]P. Virtanen, R. Gommers, T. E. Oliphant, M. Haberland, T. Reddy, D. Cournapeau, E. Burovski, P. Peterson, W. Weckesser, J. Bright, S. J. van der Walt, M. Brett, J. Wilson, K. J. Millman, N. Mayorov, A. R. J. Nelson, E. Jones, R. Kern, E. Larson, J. Carey, I. Polat, Y. Feng, E. W. Moore, and J. VanderPlas, Nat. Methods **17**, 261 (2020).
[35]M. Kunitski, S. Knippenberg, M. Gelin, C. Riehn, A. Dreuw, and B. Brutschy, Phys. Chem. Chem. Phys. **12**, 8190 (2010).
[36]Y. R. Huang, C. G. Ning, J. K. Deng, and M. S. Deleuze, Phys. Chem. Chem. Phys. **10**, 2374 (2008).
[37]J. Laane and R. C. Lord, J. Chem. Phys. **47**, 4941 (1967).
[38]M. K. Leong, V. S. Mastryukov, and J. E. Boggs, J. Mol. Struct. **445**, 149 (1998).
[39]D. Cremer, Isr. J. Chem. **20**, 12 (1980).
[40]R. Panico, W. H. Powell, and J.-C. Richer, *Nomenclature of Organic Chemistry* (Blackwell Scientific Publications, Oxford, UK, 1993).
[41]D. F. Bocian, H. M. Pickett, T. C. Rounds, and H. L. Strauss, J. Am. Chem. soc **97**, 687 (1975).

[42]M. Sagiroglugil, A. Nin-Hill, and C. Rovira, J. Chem. Phys. **163**, 124114 (2025).
[43]M. K. Jahn, D. A. Dewald, M. Vallejo-López, E. J. Cocinero, A. Lesarri, W. Zou, D. Cremer, and J.-U. Grabow, Chem. Eur. J. **20**, 14084 (2014).
[44]J.-D. Chai and M. Head-Gordon, Phys. Chem. Chem. Phys. **10**, 6615 (2008).
[45]F. Weigend and R. Ahlrichs, Phys. Chem. Chem. Phys. **7**, 3297 (2005).
[46]M. J. Frisch, G. W. Trucks, H. B. Schlegel, G. E. Scuseria, M. A. Robb, J. R. Cheeseman, G. Scalmani, V. Barone, G. A. Petersson, H. Nakatsuji, X. Li, M. Caricato, A. V. Marenich, J. Bloino, B. G. Janesko, R. Gomperts, B. Mennucci, H. P. Hratchian, J. V. Ortiz, A. F. Izmaylov, J. L. Sonnenberg, D. Williams-Young, F. Ding, F. Lipparini, F. Egidi, J. Goings, B. Peng, A. Petrone, T. Henderson, D. Ranasinghe, V. G. Zakrzewski, J. Gao, N. Rega, G. Zheng, W. Liang, M. Hada, M. Ehara, K. Toyota, R. Fukuda, J. Hasegawa, M. Ishida, T. Nakajima, Y. Honda, O. Kitao, H. Nakai, T. Vreven, K. Throssell, J. A. Montgomery, Jr., J. E. Peralta, F. Ogliaro, M. J. Bearpark, J. J. Heyd, E. N. Brothers, K. N. Kudin, V. N. Staroverov, T. A. Keith, R. Kobayashi, J. Normand, K. Raghavachari, A. P. Rendell, J. C. Burant, S. S. Iyengar, J. Tomasi, M. Cossi, J. M. Millam, M. Klene, C. Adamo, R. Cammi, J. W. Ochterski, R. L. Martin, K. Morokuma, O. Farkas, J. B. Foresman, and D. J. Fox, "Gaussian 16 Revision C.01," (2016), gaussian Inc. Wallingford CT.
[47]A. Lema-Saavedra and A. Fernández-Ramos, "A general method for constructing and searching conformations in molecular rings: From Cremer–Pople coordinates to 3D geometries," (2025), DOI: 10.5281/zenodo.17831714.
[48]K. Kakhiani, U. Lourderaj, W. Hu, D. Birney, and W. L. Hase, J. Phys. Chem. A **113**, 4570 (2009).
[49]P. M. Ivanov and E. Ōsawa, J. Comput. Chem, **5**, 307 (1984).
[50]K. B. Wiberg, J. Org. Chem. **68**, 9322 (2003).
[51]O. V. Shishkin, J. Struct. Chem. **41**, 383 (2000).
[52]S. Saebo and J. E. Boggs, J. Mol. Struct.: THEOCHEM **87**, 365 (1982).
[53]G. Favini, J. Mol. Struct.: THEOCHEM **93**, 139 (1983).
[54]F. R. Jensen and C. H. Bushweller, J. Am. Chem. Soc. **91**, 5774 (1969).
[55]F. Groenewald and J. Dillen, Struct. Chem. **23**, 723 (2012).
[56]F. A. L. Anet and I. Yavari, J. Am. Chem. Soc. **100**, 7814 (1978).
[57]I. Yavari, H. Kabiri-Fard, and S. Moradi, J. Mol. Struct.: THEOCHEM **623**, 237 (2003).
[58]O. Ermer, J. Am. Chem. Soc. **98**, 3964 (1976).
[59]W. R. Rocha and W. B. De Almeida, J. Comput. Chem. **18**, 254 (1997).
[60]U. Neuenschwander and I. Hermans, J. Org. Chem. **76**, 10236 (2011).
[61]F. Freeman and K. U. Do, J. Mol. Struct.: THEOCHEM **577**, 43 (2002).
[62]F. Freeman, J. H. Hwang, E. Hae Junge, P. Dinesh Parmar, Z. Renz, and J. Trinh, Int. J. Quantum Chem. **108**, 339 (2008).
[63]I. Yavari, D. Tahmassebi, D. Nori-Shargh, and M. Heydari, Monatsh. Chem. **127**, 1021 (1996).
[64]J. Dillen, Struct. Chem. **24**, 751 (2013).
[65]W. L. Meyer, P. W. Taylor, S. A. Reed, M. C. Leister, H. J. Schneider, G. Schmidt, F. E. Evans, and R. A. Levine, J. Org. Chem. **57**, 291 (1992).